Published in final edited form as:

J Immunol. 2020 May 15; 204(10): 2791–2807. doi:10.4049/jimmunol.1901421.

Development of interferon-stimulated gene expression from embryogenesis through adulthood, with and without constitutive MDA5 pathway activation

Laura Bankers[*], **Caitlin Miller**[*], **Guoqi Liu**[*], **Chommanart Thongkittidilok**[*], **James Morrison**[*], **Eric M. Poeschla**[*]

[*]Division of Infectious Diseases, Anschutz Medical Campus, University of Colorado Denver School of Medicine, Aurora, Colorado, USA

Abstract

Pathogen-associated molecular patterns, *e.g.* dsRNA, activate expression of interferon (IFN)-stimulated genes (ISGs), which protect hosts from infection. While transient ISG upregulation is essential for effective innate immunity, constitutive activation typically causes harmful autoimmunity in mice and humans, often including severe developmental abnormalities. We have shown that transgenic mice expressing a picornavirus RNA-dependent RNA polymerase, outside the viral context (RdRP mice), exhibit constitutive, MDA5-dependent, and quantitatively dramatic upregulation of many ISGs, which confers broad viral infection resistance. Remarkably, RdRP mice never develop autoinflammation, interferonopathy, or other discernible abnormalities. Here we used RNA-seq and other methods to analyze ISG expression across five time points from fetal development to adulthood in wild type and RdRP mice. In RdRP mice, the proportion of upregulated ISGs increased during development, with the most dramatic induction occurring two weeks postnatally. The amplified ISG profile is then maintained lifelong. Molecular pathways and biological functions associated with innate immune and IFN signaling are only activated postnatally, suggesting constrained fetal responsiveness to innate immune stimuli. Biological functions supporting replication of viruses are only inhibited postnatally. We further determined that the RdRP is expressed at low levels, and that blocking *Ifnar1* reverses the amplified ISG transcriptome in adults. In conclusion, the upregulated ISG profile of RdRP mice is mostly triggered early postnatally, is maintained through adulthood, and requires ongoing type I IFN signaling to maintain it. The model provides opportunities to study the systems biology of innate immunity and to determine how sustained ISG upregulation can be compatible with robust health.

Keywords

Antiviral innate immunity; innate immune system development; interferon-stimulated genes (ISGs); MDA5; IFNAR1; RNA-dependent RNA Polymerase (RdRP); autoimmunity; interferonopathy

Address correspondence and reprint requests to Dr. Eric M. Poeschla, Division of Infectious Diseases, University of Colorado Denver School of Medicine, Mail Stop B168, Research Complex 2, 12700 East 19th Avenue, Aurora Colorado 80045. eric.poeschla@cuanschutz.edu. Tel: 303-724-8770. FAX: 303-724-4926.

Introduction

The innate immune system is a crucial front-line barrier against pathogens. Host-encoded pattern recognition receptor (PRRs) molecules recognize molecularly conserved features of invading infectious agents, *i.e.*, pathogen-associated molecular patterns, or PAMPs (1, 2). In the case of RNA viruses, virally encoded RNA-dependent RNA polymerases (RdRPs) replicate and transcribe the viral genome, which requires the generation of double-stranded RNA (dsRNA) intermediates; these dsRNAs are an important class of PAMPs (3–5). The gene encoding the RdRP is the only universally conserved gene among RNA viruses. Importantly, unlike plants and worms, vertebrate cells do not encode RdRPs, making innate sensing of viral dsRNAs vitally specific. Recognition of cytoplasmic viral dsRNA is mediated by the RIG-I-like receptors (RLRs) MDA5, which, in general, recognizes longer dsRNAs two kb or greater (6, 7) or RIG-I, which recognizes shorter 5'-ppp-dsRNAs or 5'-pp-dsRNAs (8, 9). When they engage dsRNA, both of these sensors initiate signaling cascades through the mitochondrion-associated adaptor MAVS (10–12), which culminate in the expression of Type I interferons (IFNs) and other inflammatory cytokines in both infected and neighboring uninfected host cells (5).

The mammalian ISG activation system has evolved to enable a forceful but temporally brief interferon-stimulated gene response (13), in order to defend hosts against pathogens. The ISG response is then promptly downregulated within days to weeks, to protect against prolonged cytokine-mediated tissue inflammation as the adaptive, antigen-specific immune system takes over the task of pathogen blockade. Chronic autoinflammatory diseases often ensue when this ISG activation state is not temporally limited. Deleterious outcomes include systemic lupus erythematosus (SLE), degenerative arthritis, Aicardi-Goutieres syndrome (AGS), and Singelton-Merten syndrome (14, 15).

Informative mutant mouse models corroborate this concept, showing that constitutive activation of ISGs routinely triggers harmful autoimmune and autoinflammatory problems (16–18). The relevant murine models include gain of function (GOF) mutants of *ifih1* (MDA5) (16, 17). Chronic Type I IFN induction by *ifih1* GOF mutations such as G821S, cause lupus-like autoimmunity (17). Similar gain-of-function mutations in *ifih1* as well as mutations in other genes involved in nucleic acid metabolism, antiviral sensing, and interferon induction, cause clinically severe AGS in humans (14, 19). Also, mutations in mammalian *TREX1*, a cytoplasmic 3'−5' DNA exonuclease that metabolizes endogenous DNAs, are associated with SLE, AGS and familial chilblain lupus (16, 20–23) and this protein plays a key role in limiting HIV-1 viral cDNA-triggered immune activation as well (24–26). These and numerous similar studies underscore the importance of properly regulating innate sensing and responses to viral and endogenous nucleic acids.

We previously described a transgenic mouse that expresses the RdRP of a picornavirus (the $3D^{pol}$ protein of Theiler's murine encephalomyelitis virus, TMEV), hereafter "RdRP mice" (27). Importantly, during viral replication, members of the vast family of positive-strand RNA viruses universally sequester their RdRPs from the cytosol in cell membrane-derived replication factories. Current views suggest two main functions: biochemical concentration of viral proteins and RNAs to facilitate ordered assembly, and less demonstrated but likely

important, sequestration of viral dsRNA intermediates in order to minimize detection by cytosolic dsRNA sensors (28–31). Single-stranded (+) RNAs synthesized by the RdRP can then be emitted via small pores to the cytoplasm to participate in ribosomal translation and viral assembly.

In contrast, RdRP mice ectopically express the RdRP in an unsequestered manner, *i.e.*, outside the viral context (27). The protein is diffusely distributed in the cell (C. Miller, unpublished data). Thus, its dsRNA products are presumably directly exposed to cytosolic sensors such as RIG-I-like receptors (RLRs). Corroborative experiments in human cells with catalytic center mutants showed that the ISG upregulation requires a catalytically active RdRP. Whole-genome mRNA microarrays demonstrated that these mice exhibit systemic, quantitatively dramatic induction of numerous ISG mRNAs (corroborated at the protein level) (27). RdRP mice are also broadly resistant to infection by phylogenetically diverse RNA and DNA viruses such as TMEV itself, encephalomyocarditis virus, vesicular stomatitis virus, and pseudorabies virus (27, 32, 33). A series of six knockout mouse crosses demonstrated that both ISG induction and resistance to viral infection depend on *Mda5*, *Mavs*, and *Ifnar*. That ISG activation is dependent on the dsRNA sensor *Mda5* led to the hypothesis, and confirmation, that cells of RdRP mice have elevated levels of dsRNA, presumed to be transcribed from host cellular RNA (27). While these mice display extensive, permanent remodeling of the innate immune system, characterized by constitutive, quantitatively dramatic, *Ifnar*-dependent upregulation of many ISGs, they do not have elevated interferon mRNAs and do not experience any autoimmune or autoinflammatory problems, as would be predicted strongly by both mouse and human disease models (17–19). Surprisingly and intriguingly, they are indistinguishable from wild-type mice in tissue morphology and histology, habitus, weight gain, fertility, behavior, and longevity (27).

Organismal induction and responsiveness to Type I interferons appears to be especially complex during pregnancy. Prevention of maternal immune responses to the semi-allogeneic fetus necessitates a period of dampened inflammation during pregnancy, though immune responses are still required for fetal protection from pathogens. This results in a dynamic, carefully balanced responsiveness of both maternal and fetal innate immune systems to appropriate ligands. Inappropriate or excessive induction of type I interferons due to infection or autoimmune disorders has deleterious effects on pregnancy outcomes (34, 35). An elevated interferon response has also been implicated in the disorders associated with trisomy 21 (36). Administration of the dsRNA mimetic poly(I:C) to pregnant mice induced fetal demise in an *Ifnar1*-dependent manner, demonstrating both that mice remain responsive to RIG-I-like receptor signaling during pregnancy and that subsequent induction of type I interferons has disastrous effects on the developing fetus (35, 37). Whether the RdRP transgene is expressed – and subsequently produced dsRNAs are sensed – throughout mouse development remain main unanswered questions in unravelling the RdRP mouse's singular features and explaining why the large ISG elevations observed in adult animals are not embryonic lethal and are also compatible with lifelong robust health.

Here, because embryogenesis requires tightly orchestrated regulation of many interacting genes and molecular pathways, we used RNA-seq and other methods to compare patterns of

gene expression between wild-type and RdRP mice during development. We find that a dramatic increase in the expression of ISGs occurs in RdRP mice within the first two weeks of post-natal life, which is then maintained through adulthood. In contrast, at fetal and neonatal timepoints, the mice have altered gene expression profiles but no induction of classical type I interferon pathways. The mechanism behind the sustained ISG elevation involves ongoing (post-developmental) type I IFN signaling, as blocking *Ifnar1* reverses it in adults. The RdRP was expressed at all time points, and even in the presence of this innate immune ligand producing factor, fetal mice do not mount a classical ISG response.

Materials and Methods

Mice

All animals were cared for according to local, state, and federal regulations in accordance with protocols approved by the University of Colorado Denver Institutional Animal Care and Use Committee and consistent with National Institutes of Health guidelines for the care and use of animals. The WT and RdRP-transgenic mice used in the RNA-seq experiments in this study are C57BL/6. WT and RdRP mice on both the C57BL/6 and FVB backgrounds were used for the RT-qPCR experiments to confirm RNA-seq results. C57BL/6 and FVB RdRP mice are described in (27). RdRP transgenic mice were maintained as homozygotes on all mouse strain backgrounds used in this work.

RNA-seq sample collection and preparation

Brain tissue was collected from four littermate WT and four littermate RdRP mice at each of five time points (40 samples): embryonic day 10.5 (E10.5), embryonic day 14.5 (E14.5), neonates within 12 hours of birth (neonatal), two weeks post-natal (2wk), and 10 weeks post-natal (10wk). To obtain each set of littermates, pairs of male and female mice were put into individual cages in the evening and each subsequent morning the females were checked for the presence of a copulatory plug, indicating that mating had occurred. The morning in which a copulatory plug was found was called embryonic day 0.5 (E0.5, or 0.5 days post coitum (dpc)) (38, 39) and prenatal time points were collected on embryonic days 10.5 and 14.5. E10.5 was chosen as the earliest prenatal time point because E10.5 was the earliest point during embryonic development in which we could reliably harvest brain tissue. E14.5 was chosen because previous studies have shown that at this point in development key inflammatory response and innate immune genes such as *Tlr2* and *Tlr4* begin to reach detectable expression levels (40), and dysregulation of Interferon-β in E14.5 *Dnase2a*−/− mice leads to lethal anemia (41), meaning that this time point may be interesting in regards to evaluating the intersection of embryonic development and innate immune system function (42).

For the two prenatal time points, pregnant females were euthanized with isoflurane followed by cervical dislocation. Fetal mice were dissected out of the female, euthanized by decapitation, and the brain tissue was harvested using a dissecting microscope. Brain tissue was also harvested from neonates, and post-natal two-week and 10-week-old mice after euthanasia with isoflurane followed by cervical dislocation and decapitation. Brain tissue

was immediately placed in TRIzol Reagent (Invitrogen, USA) and stored at −80°C until RNA extraction.

RNA extraction and sex determination for RNA-seq

For each sample, brain tissue was homogenized in 1 mL of TRIzol Reagent (Invitrogen, USA) using a QAIGEN TissueLyser LT (QAIGEN, USA). RNA was extracted following the TRIzol protocol with manufacturer's instruction (Invitrogen, USA). Following RNA extraction, RNA concentration and quality was assessed using a Nanodrop 1000 (ThermoFisher Scientific, USA).

Furthermore, in order to rule out potential biases due to sex, we isolated tissue and extracted RNA from two males and two females for both WT mice and RdRP mice for each of the five time points. Because it is not possible to morphologically determine sex at the prenatal and neonatal time points, we PCR amplified a Y chromosome marker, a 362 bp portion of the *Sry* gene, to determine which prenatal and neonatal mice were males. First, we used the QuantaBio qScript cDNA SuperMix (QuantaBio, USA), following manufacturer's instructions, to synthesize cDNA from a portion of each RNA extraction. PCR reactions were set up using Apex™ Taq DNA polymerase 2.0x Master Mix (Genesee Scientific, USA), ~20 ng of cDNA template, and the following primers amplify SRY: forward 5'-ATGGAGGGCCATGTCAA-3' and reverse 5'-CATACAGGCAAGACTGGAGTAGAGCTG-3'. Male mice were identified by successful amplification of the portion of *Sry*, as determined by the presence of a band in a 1% agarose gel. For all samples that initially failed to amplify *Sry*, PCR and gel electrophoresis were replicated a second time to confirm that the sample was female, as opposed to an initially failed PCR reaction.

Library preparation and RNA-seq

Library preparation and RNA-sequencing (RNA-seq) were performed by Beijing Genomics Institute (BGI, Shenzhen, China). Briefly, DNaseI was used to remove genomic DNA from each of the 40 RNA extractions (Invitrogen, USA). Then mRNA enrichment was performed using oligo(dT) magnetic beads. Next, RNA was sheared, and random primers were used to reverse transcribe the RNA into cDNA. This was followed by end repair, poly-A and adaptor ligation, brief PCR amplification, single strand separation and cyclization, and DNA nanoball synthesis (BGI, Shenzhen, China). The quality of each library was assessed using an Agilent 2100 Bioanalyzer (Agilent, Technologies, CA, USA). The BGIseq-500 platform was then used for 50 bp single-end RNA sequencing (BGI, Shenzhen, China).

RNA-seq gene expression analyses

After RNA-sequencing, we assessed the quality of raw reads using FastQC version 0.11.5 (43) and used FASTX-Toolkit version 0.0.13 (44) to filter poor quality reads, requiring a mean Phred quality score per read of at least 20. Post-filtering read quality was re-assessed with FastQC. We obtained a mean number of raw reads per sample of 26,706,447.03 (SD ± 1,810,120.84). After filtering we retained a mean number of reads per sample of 26,701,850.18 (SD ± 1,808,541.10). Raw sequencing data have been deposited on NCBI Sequence Read Archive (SRA; https://www.ncbi.nlm.nih.gov/sra) and are publicly available

under BioProject PRJNA609137, BioSample accessions SAMN14232667-SAMN14232676, and SRA accessions SRR11195695-SRR11195704.

We used STAR 2.6 (45) to map the filtered reads to the mouse mm10 genome assembly (obtained from iGenomes, Illumina, Inc., USA) with the RdRP sequence appended to end of the fasta genome file and the GTF annotation file in order to assess expression of all annotated genes in the mouse genome and the RdRP transgene simultaneously. We then used SAMtools view to convert the STAR output sam file into bam format (46). Next, we used Picard Tools to process the bam files (47). This included adding read groups to each bam file with AddOrReplaceReadGroups, marking and removing PCR duplicates that result from library preparation with MarkDuplicates, and then sorting the bam file by genomic coordinates using SortSam. After processing the bam files, we assessed quality statistics of each bam file using SAMtools samstat (46). After processing, a mean of 26,304,385.43 (SD ± 1775680.15) reads per sample mapped to the reference genome including the mouse mm10 assembly and the RdRP sequence (~98.51% of reads per sample).

In order to evaluate patterns of gene expression between WT and RdRP mice within and among time points we used the Tuxedo pipeline (48–50). First, we used Cufflinks to quantify transcript abundance for each sample. Cuffmerge was then used to combine the individual Cufflinks GTF outputs into a single merged GTF file. We used CuffDiff to perform differential gene expression comparisons with an FDR cutoff of 0.05 and Benjamini-Hochberg correction for multiple tests and a minimum of five-fold differences in expression as cutoffs for significance (Table SI). In order for expression differences to be compared, we required a minimum Fragments per Kilobase per Million Reads Mapped (FPKM) of five to reduce false positives. The mean FPKM values across the four biological replicates for WT and RdRP mice at each of the five time points can be found in Table SII. We compared patterns of gene expression in two ways: 1) pairwise comparisons of WT mice *vs.* RdRP mice within each time point (*e.g.* E10.5 WT mice *vs.* E10.5 RdRP mice), and 2) time series gene expression comparison, performed separately for WT mice and RdRP mice, in which expression for a given time point is compared to the immediately previous time point (*e.g.* for RdRP mice: E10.5 *vs.* E14.5, E14.5 *vs.* neonatal, neonatal *vs.* 2wk, 2wk *vs.* 10wk). The R packages cummeRbund (51) and Plotly (52) were used to visualize our results.

In silico functional analyses of differentially expressed genes

In order to determine the functions of differentially expressed genes (DEGs), we first compared our DEGs to the Interferome Database (53) to assess the proportion of DEGs that represent known Interferon stimulated genes (ISGs) for both WT mice and RdRP mice and at each time point. In particular, we identified genes whose expression levels have been shown to respond to type I IFNs in mice and mouse cell line systems. Next, we used Ingenuity Pathway Analysis (54) to perform Canonical Pathways, Upstream Regulators, and Diseases and Biological Functions analyses. Canonical Pathways analyses were used to identify molecular pathways with evidence for activation or inhibition in our data, pathways are then grouped into broader functional categories based on the IPA knowledge base. The Canonical Pathways analysis uses the activation z-score and *p*-value of overlap, as

implemented in IPA, the z-score compares patterns of gene expression in our datasets as well as information from the IPA knowledgebase to determine if a pathway is likely to be activated (z-score ≥ +2) or inhibited (z-score ≤ −2). The *p*-value of overlap evaluates the proportion of genes in the dataset that overlap with genes known to be involved in a particular pathway (*p*-value ≤ 0.05 indicates a significant overlap between genes in our dataset and genes involved in a given pathway based on Fisher's Exact Tests with Benjamini-Hochberg multiple test correction). We also performed the IPA Upstream Regulators analysis, which identifies differentially expressed genes in the dataset that have predicted activation or inhibition effects on other genes and pathways in the dataset. Diseases and Biological Functions analyses were used to identify associations between expression patterns in our datasets and known Diseases and Biological Functions. The *p*-value of overlap of genes in our dataset relative to genes involved in a particular disease or biological function was used to determine if that disease or biological function is over- *vs.* under-represented in our data, and activation z-scores were used to determine whether those Diseases and Biological Functions are likely to be activated or inhibited. Finally, we corroborated the IPA functional enrichment analyses by also performing gene ontology (GO) enrichment analyses (55, 56) using DAVID with Benjamini-Hochberg multiple test correction, and otherwise default parameters (57, 58).

MAR1-5A injection of mice

Adult, 6-8-week-old C57BL/6 RdRP or WT mice of mixed sex were administered MAR1-5A or IgG control (Leinco Technologies, Inc.) intraperitoneally via two injections. Based on manufacturer recommendations, an initial dose of 2.5 mg/mouse was administered, with a follow-up dose of 0.5 mg/mouse on day five after initial injection (Fig 5A). Mice were euthanized via CO_2 euthanasia and cervical dislocation on day eight after initial injection and brain, liver, and spleen samples were removed and divided evenly in two. Half of each sample was placed directly into Trizol (Invitrogen). The remaining half sample was processed through 0.70 μM nylon cell strainers (59) to create a single cell suspension. Cells were lysed for western blot in 1x RIPA buffer containing protease inhibitor (Roche Complete ULTRA tablets, Roche).

RT-qPCR of representative ISGs

Total RNA was extracted from whole brain, liver, or spleen tissue of WT and RdRP mice with either the RNeasy kit (QIAGEN, USA) or Trizol reagent (Invitrogen) according to manufacturer's instructions. Following RNA extraction, RNA was reverse transcribed with an oligo-dT and M-MLV first-strand synthesis kit for RT-PCR (Roche, USA) or using Maxima H Minus First Strand cDNA Synthesis Kit (Thermo Scientific) according to kit instructions. Reverse transcription reactions were performed on a Mastercycler (Eppendorf, USA). Next, qPCR reactions were performed with iQ-SYBR Green Supermix (BioRad, USA) or using 2x qPCR Master Mix Green (Apex) on a CFX96 Real-time system. Primer sequences for *Ddx58* (RIG-I), *Ifit1*, *OasL2*, and *Isg15* have been reported (27). Primer sequences for *Ifih1* (MDA5) are as follows: forward 5'-TCACTGATCTGCCCTCTCCT-3' and reverse 5'-CCTTCTCGAAGCAAGTGTCC-3'. PCR primers were synthesized by IDT (Integrated DNA technologies, USA). All samples were amplified in duplicate or triplicate wells. Relative gene expression was determined using the $2^{-\Delta\Delta CT}$ method, with *Gapdh* as the

internal control. Data were analyzed using Graphpad Prism 8.0 and are presented as mean ± SEM. For time course analysis of qPCR data, a two-way ANOVA was used to determine significance. For anti-IFNAR qPCR data analysis, a one-way ANOVA followed by a Tukey test was used to determine significance thresholds.

Immunoblotting

Samples were prepared and run as described (27). Briefly, protein concentration was determined by Bradford reaction (Bio-Rad) according to manufacturer instructions. 35 ug/well were prepared in lysis buffer and 6X reducing SDS sample buffer (Bio-Rad) and boiled for 5-10 minutes prior to loading. Samples were run on 4-15% gradient SDS-PAGE gels (Bio-Rad), transferred to polyvinylidene difluoride membrane (Bio-Rad) and blocked for at least one hour at room temperature in 5% milk in tris-buffered saline containing Tween20 (TBS-T, 0.1% Tween20). Rabbit polyclonal antibodies for ISG15, RIG-I, and actin (Cell Signaling) and goat anti-rabbit secondary detection antibody conjugated to horseradish peroxidase (Millipore) were described (27). Western blots were developed with Immobilon Crescendo Western HRP substrate (Millipore).

Results

Pairwise analysis: the characteristic ISG induction of the RdRP mouse occurs postnatally

In order to determine whether and how expression of the RdRP transgene influences gene expression (particularly ISG expression) throughout the course of development, RNA-seq was used to compare patterns of gene expression between wild-type (WT) and RdRP transgenic C57BL/6 mice at five different developmental time points (E10.5, E14.5, neonatal, 2wks after birth, and 10wks after birth). In addition, we wished to chart the normal developmental ISG transcriptional program that occurs in WT mice. Whole brain tissue was chosen as it showed substantial ISG elevations in previous work (27) and neurogenesis is detrimentally altered by a range of disease states associated with maternally or fetally upregulated ISGs (34, 35). First, we used CummeRbund to generate a multidimensional scaling plot (MDS), which clusters samples based on their gene expression profile, such that samples with more similar gene expression profiles will cluster closer together in the plot space. The samples cluster first by developmental time point, and then by condition (condition refers to WT *vs.* RdRP throughout), indicating that developmental time point is a strong driver of gene expression patterns among samples (Fig 1). Furthermore, the 2wk and 10wk time points cluster close to each other indicating that these two time points have the most similar gene expression profiles.

Next, we performed pairwise comparisons of RdRP mice relative to WT mice within each of the five time points. From these analyses we identified between 16 and 49 differentially expressed genes (DEGs) with at least five-fold differences in expression between WT and RdRP mice at all developmental time points, many of which represent known ISGs (Table I). A five-fold cutoff was chosen because of the dramatic expression differences observed in mRNA microarrays in Painter et al (27). Analyses performed with a minimum of two-fold expression differences, yielding 49-494 DEGS per time point, can be found in the supplement and show qualitatively similar patterns (Table SI). The DEGs at all time points

included ISGs, the expression of which was previously shown to be genetically dependent on the dsRNA-sensing proteins MAD5 and MAVS (27). The peak of ISG induction at the 2wk time point suggests that dsRNA sensing and downstream signaling is dampened during fetal development. In support of this, most canonical ISGs (*e.g.* ISG15 and Stat1) (60–65) are induced in two-week and 10-week old RdRP mice, in which > 75% of five-fold upregulated genes are ISGs (Fig 2; Table I, Table SI). Furthermore, the interferon-regulatory factors *Irf7* and *Irf9* – transcription factors that bridge pattern-recognition receptor signaling and type I IFN induction (66) – were only found to be differentially expressed in RdRP mice at two- and 10-weeks of age (Table SI). We cannot definitively conclude whether these gene expression changes are solely due to sensing of RdRP-generated dsRNA and do not reflect an additional contribution from a response to the RdRP protein itself. That is unlikely however, as in addition to the MDA5-MAVS pathway dependence noted above, a catalytic center mutant RdRP did not trigger ISG elevations in sensing-competent human THP-1 monocytes (27).

We also evaluated whether the DEGs that were up or downregulated at one time point in RdRP mice relative to WT mice showed that same expression pattern in any of the other four time points. This analysis showed that the two postnatal time points (2wk, 10wk) have more DEGs showing the same expression pattern than any other comparison among time points. In particular, at the 5x differential expression cutoff, 2wk and 10wk RdRP mice show the same expression patterns for 20 DEGs, all of which are upregulated ISGs. Neonates, 2wk and 10wk show the same expression patterns for four DEGs (all upregulated, one ISG), and all other possible comparisons have no more than one DEG in common. Taken together, these results indicate that, although there are clearly gene expression differences between WT and RdRP mice during fetal development (a time series analysis follows below for both conditions), the primary signal of ISG induction in RdRP mice occurs overwhelmingly postnatally. Finally, as expected, FPKM of the RdRP transgene itself was zero for all WT time points, indicating no contamination with RdRP mice or spurious mapping. For RdRP mice, mean FPKM (+/−SD) values for the RdRP transgene mRNA were 3.534 (+/− 0.239) at E10.5, 4.551 (+/− 0.702) at E14.5, 3.804 (+/− 1.138) at neonatal, 0.921 (+/− 0.167) at 2wk, and 1.288 (+/− 0.696) at 10wk, meaning that the RdRP transgene is expressed at all time points, but expression was generally low compared with all expressed cellular gene transcripts (mean FPKM 23.026 +/− 157.068) and consistent between biological replicates. This result indicates impressive potency for this transgene.

To confirm the RNA-seq analyses by RT-qPCR, we measured three canonical ISGS (*Ifit1*, *Oasl2*, and *Isg15*), as well as the two main dsRNA-sensing RLRs *Ddx58* (RIG-I) and *ifih1* (MDA5), which are themselves ISGs. Consistent with the RNA-seq data, we observe a significant increase in expression of all three ISGs in 2wk and 10wk RdRP mice, relative to WT (Fig 3). During prenatal and neonatal timepoints, expression of the ISGs and RLRs are indistinguishable from WT mice (Fig. 3; Table SII). In concert with postnatal ISG induction, RLR expression increases. However, in the RNA-seq data only modest increases (not statistically significant, except for *Ddx58* at 10wk) are observed compared to the RT-qPCR because these genes do not meet the minimum FPKM of five and fold change requirements (5x; see Methods). This difference in the RNA-seq vs. RT-qPCR is likely due to the combination of low FPKM values in the RNA-seq and the wider dynamic range of qRT-

PCR, which allows for better differential expression detection of lowly expressed genes. Even so, this pattern of low RLR expression at all time points (FPKM range of 0.34-4.48 and 0.35-1.04 for RdRP and WT mice across all time points, respectively, Table SII) and minor upregulation in RdRP relative to WT mice (*ifih1* upregulated by 3.03x at 2wk and 4.11x at 10wk; *Ddx58* upregulated by 3.74x at 2wk and 6.44x at 10wk, Table SI) is compatible with particular potency for the RLRs in mediating induction of ISGs. Alternatively, their levels may not be determinative for MAVS-dependent broad ISG upregulation and their transcripts may be modestly elevated simply on the basis of being ISGs themselves. As of yet, what may be constraining RLR expression early on, which may have effects on ISG induction, remains unknown.

In addition, in order to discount the possibility that the C57BL/6 mice used in this study have unique developmental responsiveness to RdRP-generated innate immune stimuli, RdRP mice on the FVB background were also examined. FVB mice are immunocompetent and are known to mount an especially vigorous innate immune system response to the fungal pathogen *Pneumocystis* (67). We examined the expression levels of the same set of genes by RT-qPCR from brain tissue of neonatal mice and post-natal mice from each of weeks one through five. Consistent with the C57BL/6 data, the activation of ISGs in FVB-RdRP mice occurs postnatally (Fig S1). Similar to what we observed in C57BL/6 RdRP mice, we observed pronounced induction of ISGs, including RLRs, beginning at two weeks postnatal, compared with one week and neonatal, which continues to increase up to five weeks postnatal (Fig S1). Together with the RNA-seq data, these RT-qPCR results confirm that RdRP-mediated induction of ISGs in RdRP mice begins its major ramping up shortly after birth, and that this upregulation is mouse strain-independent.

Innate immune Canonical Pathways and Biological Functions are enriched and activated in RdRP mice postnatally

We identified seven Ingenuity Pathway Analysis (IPA) Canonical Pathways (54) that had *(i)* significant *p*-values of overlap between genes in our dataset and genes involved in particular Canonical Pathway, and *(ii)* significant evidence for activation (six Canonical Pathways) or inhibition (one Canonical Pathway) based on activation z-scores, in at least one of the pairwise comparisons (Table II). In E10.5 RdRP mice relative to E10.5 WT mice, there were five activated Canonical Pathways and one inhibited Canonical Pathway. Two of the five activated Canonical Pathways and the single inhibited Canonical Pathway are in the Intracellular and Second Messenger Signaling category (RhoA Signaling, Signaling by Rho Family GTPases, RhoGDI Signaling). Rho GTPase-mediated signaling is involved in diverse cellular function and maintenance-related processes ranging from cellular proliferation, differentiation, and migration to apoptosis and tissue development (68). Some evidence suggests that Rho GTPases, such as RhoA, are involved in IFN-γ-related immune regulation (69–71), although our previous work has shown that knock out of the IFN-γ receptor (*Ifngr1*) had no effect on the ISG profile of RdRP mice (27). The other activated Canonical Pathways are in the categories of Cellular Growth, Proliferation, and Development (pathway: ILK Signaling), Organismal Growth and Development (pathway: Actin Cytoskeleton Signaling), and Neurotransmitters and Other Nervous System Signaling (pathway: Regulation of Actin-based Motility by Rho). All six activated and inhibited

Canonical Pathways have four molecules in common (*Acta1*, *Actc1*, *Myl1*, and *Myl4*), which is consistent with their interrelated functions.

There were no significant associations between the dataset and IPA Canonical Pathways for either E14.5 RdRP mice relative to E14.5 WT mice, nor neonatal RdRP mice relative to neonatal WT mice. For both 2wk RdRP mice relative to 2wk WT mice and 10wk RdRP mice relative to 10wk WT mice, we observed a significant *p*-value of overlap and positive activation z-score for the Interferon Signaling pathway. These are also the only two time points for which IPA identified upstream regulators with known activation/inhibition effects on the enriched pathways and that were differentially expressed in our dataset (Table II), all of which represent important known regulators of Interferon Signaling and are ISGs themselves. This result provides further evidence that the strongest ISG induction primarily occurs in the two latest time points because we do not observe significant induction of the Interferon Signaling pathway until the 2wk and 10wk time points.

We also identified 13 IPA Diseases and Biological Functions that were both *(i)* enriched based on the *p*-values of overlap between genes in the dataset and genes associated with a particular disease or biological function in the IPA knowledgebase (Table III), and *(ii)* had significant activation z-scores (three activated and 10 inhibited), in at least one of the five time points. We also identified 40 significantly enriched Gene Ontology (GO) terms using DAVID. In E10.5 RdRP mice relative to E10.5 WT mice, we observed four enriched Diseases and Biological Functions with significant evidence for inhibition and were related to developmental abnormalities (Hypoplasia of Organ), and mortality (Organismal Death, Perinatal Death, and Neonatal Death) as well as enrichment of development (particularly neural development) and transcription related GO terms. Similar to the Canonical Pathways analysis, we did not observe any significantly enriched and activated/inhibited Diseases and Biological Functions or GO terms in E14.5 RdRP mice relative to E14.5 WT mice, and only ribosome-related GO terms were enriched in neonatal RdRP mice relative to neonatal WT mice.

Considering Diseases and Biological Functions in 2wk RdRP mice relative to 2wk WT mice, only Immune Response of Cells was significantly activated, and six Diseases and Biological Functions – four of which can be inferred to directly support infection by pathogens – were significantly inhibited (Bacterial Infections, Viral Infection, Infection of Mammalia, Quantity of IL-12 in Blood, Morbidity & Mortality, and Organismal Death). We observed three enriched and activated Diseases and Biological Functions in 10wk RdRP mice relative to 10wk WT mice (Immune Response of Cells, Leukocyte Migration, and Migration of Cells), and five were enriched and inhibited (Infection of Mammalia, Organismal Death, Quantity of IL-12 in Blood, Replication of Vesicular Stomatitis Virus, and Viral Infection). Importantly, five Biological Functions showed the same patterns of activation/inhibition at both the 2wk and 10wk time points. Similarly, seven innate immune system-related GO terms were enriched in both 2wk and 10wk time points, and additional antigen processing and presentation GO terms were enriched at 10wk (Table III). Consistent with patterns of ISG induction and the activation/inhibition of Canonical Pathways, we did not observe significant activation of immune-related Biological Functions, or significant inhibition of infection/viral replication functions until the 2wk and 10wk time points.

Time series analysis: ISG induction in RdRP mice is maintained postnatally

Next, we performed time-series gene expression comparisons. For these analyses, gene expression differences in a given time point are evaluated relative to the immediately prior time point (*e.g.* E14.5 relative to E10.5). The analyses were done separately for WT mice and RdRP mice to determine how gene expression patterns change over time in each condition, and then the results of these two separate analyses were compared. Like the pairwise gene expression comparisons, we used a 5x expression difference cutoff, and analyses performed with a minimum of 2x expression differences show qualitatively similar patterns (Table SI).

Across each of the four comparisons (E14.5 relative to E10.5, neonatal relative to E14.5, 2wk relative to neonatal, and 10wk relative to 2wk), we identified 3,977 DEGs that showed the same directional changes in expression between time points in both WT mice and RdRP mice (at least 2x differences in expression), of which 662 were differentially expressed by at least 5x in both WT mice and RdRP mice. These genes represent genes for which expression patterns change during development and which are not markedly altered by RdRP transgene expression. Thus, they provide a data-minable resource for tracking pre- and post-embryonic developmental changes in mice generally (Table IV).

There were 201 and 86 genes that were differentially expressed among time points in RdRP mice and WT mice, respectively, and were either only differentially expressed in that condition (*e.g.* only upregulated in RdRP mice at E14.5 relative to E10.5), or that showed differing expression patterns across conditions/time (*e.g.* upregulated in RdRP mice at E14.5 relative to E10.5, but upregulated in WT mice at neonatal relative to E14.5) (Table SI). Thus, this latter set of 287 differentially expressed genes likely represent genes for which expression is, at least in part, governed by the presence or absence of RdRP transgene expression. We therefore focused additional analyses on these genes (Fig 4).

While a small number of differentially expressed ISGs are observed between each time point for WT mice, few represent canonical ISGs (*e.g. Ifit1*, *Isg15*) (27, 60–65). Similarly, in RdRP mice, differentially expressed ISGs are observed between each time point. However, there is a distinct induction of canonical ISGs (*e.g. Ifi27*, *Ifit1*, *Isg15*) in 2wk RdRP mice relative to neonatal RdRP mice. Furthermore, there are only 10 DEGs in 10wk RdRP mice relative to 2wk RdRP mice (three ISGs; one upregulated, two downregulated), indicating that the gene expression profiles of these time points are highly similar, *i.e.*, most ISGs that increase in expression in 2wk RdRP mice relative to neonatal RdRP mice do not significantly change expression levels in 10wk RdRP mice relative to 2wk RdRP mice. In other words, ISG induction is primarily instigated and maintained postnatally, and the first two weeks of life after birth is the most critical transition period. Teleologically, this new readiness to react to dsRNA may reflect an abrupt need for defense against RdRP-encoding viruses that are absent from the intrauterine milieu (see Discussion). (Fig 4; Table SI).

The ISG state is reversible in adult mice: neutralization of IFNAR signaling confirms active Type I IFN signaling is required to maintain the ISG signature

A previous cross of RdRP mice with *Ifnar1*-knockout mice showed that the type I interferon receptor is required for the elevated ISG phenotype (27). However, whether receptor signaling is merely required developmentally, and this hardwires the augmented ISG transcriptome for the life of the animal, was not determinable from the *Ifnar1* −/− cross. Notably, neither the Ifnα nor Ifnβ mRNAs were upregulated in microarray profiling of adult RdRP mouse spinal cord tissues in which ISG mRNAs were highly elevated; basal plasma type I IFN protein levels were also not elevated (27). Moreover, RdRP mice displayed attenuated type I IFN induction following administration of the dsRNA analogue, poly(I:C) and in RdRP-expressing human THP-1 monocytes, neither human Ifnα nor Ifnβ mRNAs were significantly upregulated despite ISG mRNA induction of up to several hundred fold (27). In the present study, RNA-seq and qPCR comparisons across developmental stages indicate that the RdRP-dependent ISG signature occurs postnatally by two weeks of age and is then maintained. To determine whether active type I interferon signaling is required for the postnatal maintenance, we tested whether disrupting *Ifnar1* signaling could neutralize this ISG signature in adult mice. We injected 6-8-week-old mice intraperitoneally with MAR1-5A, a commonly used antibody that neutralizes the receptor and prevents signaling, or a matched IgG control antibody. Mice were given a high, saturating dose of the antibody, since every cell will express the IFNAR receptor, followed by a lower, maintenance dose five days later (Fig. 5A). Local tissue at the site of antibody administration (liver and spleen) and brain (parallel to other experiments presented here and in previous studies) were harvested for qPCR and western blot analysis of RdRP-driven ISGs. Local tissue was harvested in addition to brain, since it was unclear if the α-IFNAR antibody would transit to the brain via an intraperitoneal injection. Nevertheless, we observed a clear, striking reduction in the representative ISGs *Ifit1*, *Isg15*, and *Oasl2* in the brain, liver, and spleen after MAR1-5A administration, but not with the IgG control (Fig 5B–D). We also examined expression of the RLRs *Ifih1* (MDA5) and *Ddx58* (RIG-I). We observed a slight upregulation of both RLRs in RdRP mice in almost all of the tissues examined, which is to be expected since they are known ISGs (Fig 5B–D). Treatment of RdRP mice with MAR1-5A reduced expression of *Ifih1* (MDA5) and *Ddx58* (RIG-I) in the liver and *Ifih1* (MDA5) in the spleen (RIG-I was not found to be upregulated in splenic mRNA in RdRP mice) (Fig 5C, D). Both *Ifih1* (MDA5) and *Ddx58* (RIG-I) trended toward a decrease in expression in brain as well (Fig 5B), but this did not reach statistical significance. These definitive results indicate that the RdRP acts in diverse organs to induce an ISG response that requires persistent type I IFN receptor signaling and confirm that RdRP activity is not brain specific.

To further validate these results, we also measured protein levels of the representative ISG, ISG15, and the RLR RIG-I in the brain, liver, and spleen by western blot. Consistent with the qPCR data, we observe a notable decrease in ISG15 protein levels in all tissues after MAR1-5A administration (Fig 5E). Expression of RIG-I also decreased in the brain and to a lesser extent in the spleen and liver after MAR1-5A treatment (Fig 5E). RIG-I is a weakly induced ISG and thus we would not expect as dramatic of a decrease in protein levels with MAR1-5A treatment as a strongly induced ISG like ISG15. Together, these data support the

RNA-seq and qPCR data, indicating that the RdRP-dependent ISG signature is established postnatally in diverse tissue environments and may not require prenatal programming (or the latter is not sufficient for adult maintenance). We also infer that RdRP catalysis in adult mice results in tonic IFN signaling of an autocoid or paracrine nature that is required to maintain ISG production. The ability to transiently neutralize the ISG signature in adult mice is consistent with accumulated evidence that the RdRP is consistently expressed and produces dsRNA throughout the lifetime of the animal.

RdRP mice exhibit postnatal activation and maintenance over time of cellular immune response-related Canonical Pathways and Biological Functions

We identified Canonical Pathways with significant evidence for activation or inhibition across the developmental time series and identified upstream regulator genes with known activation/inhibition effects on each pathway or on DEGs within differentially regulated pathways. Similar to the time series gene expression analyses, we did this by performing IPA Canonical Pathways analysis for each time point relative to the previous time point, separately for WT and RdRP mice (*e.g.* E14.5 relative to E10.5). In particular, we identified the Canonical Pathways in which patterns of activation or inhibition changed among time points and that differed between WT mice and RdRP mice (*e.g.* a Canonical Pathway that was inhibited in E14.5 RdRP mice relative to E10.5 RdRP mice but was not inhibited in the corresponding WT comparison). We identified 19 Canonical Pathways with significant *p*-values of overlap and z-scores that showed differing activation/inhibition patterns across the time series between WT mice and RdRP mice, representing Canonical Pathways that are likely relevant to the RdRP phenotype (Table V).

Specifically, relative to E10.5 RdRP mice, E14.5 RdRP mice inhibit three Canonical Pathways in the categories of Intracellular and Second Messenger Signaling (RhoA Signaling), Cellular Growth, Development, and Proliferation (ILK Signaling), and Cell Cycle Regulation (Mitotic Roles of Polo-like Kinases) (Table V). On the other hand, of the five Canonical Pathways that are activated in E14.5 RdRP mice relative to E10.5 RdRP mice, one is in the Intracellular and Second Messenger Signaling category (α-Adrenergic Signaling), two are in the Cell Cycle Regulation category (Cell Cycle: G2/M DNA Damage Checkpoint Regulation and CDK5 Signaling), three are in the Nervous System Signaling category (GnRH Signaling, CDK5 Signaling, Ephrin Receptor Signaling), and one is in the Organismal Growth and Development categories (Ephrin Receptor Signaling). We also identified eight regulators among these pathways, four of which represent ISGs (Table V). There is one Canonical Pathway that is activated in neonatal RdRP mice relative to E14.5 RdRP mice, in the Intracellular and Second Messenger Signaling and Cancer categories (ERK/MAPK Signaling); however, no Upstream Regulators were identified. Importantly, in 2wk RdRP mice relative to neonatal RdRP mice we observe activation of two Canonical Pathways in the Cellular Immune Response categories: Interferon Signaling (also in the Cytokine Signaling category), and Neuroinflammation Signaling Pathway (also in the Nervous System Signaling category). We identified 10 upstream regulators of which eight are known ISGs, and four of which are known to regulate both pathways (Table V). Moreover, there are no significantly activated or inhibited Canonical Pathways in 10wk RdRP mice relative to 2wk RdRP mice providing further evidence that the gene expression

profiles of these two time points are highly similar and that ISG induction occurs after birth by two weeks of age and is then maintained through at least 10 weeks of age (Table V).

There are also several Canonical Pathways that exhibit significant evidence for activation or inhibition across the WT time series that do not show evidence of activation or inhibition among the RdRP mice (Table V). In E14.5 WT mice relative to E10.5 WT mice we observed the inhibition of one Canonical Pathway in the Cellular Stress and Injury category (GP6 Signaling). In this comparison we also find the activation of four Canonical Pathways: two in Intracellular and Second Messenger Signaling (Gαq Signaling and cAMP-mediated Signaling), and two Canonical Pathways in the Nervous System Signaling categories (Amyotrophic Lateral Sclerosis Signaling, which is also associated with disease, and Neuroinflammation Signaling Pathway, which is also in the Cellular Immune Response category). Neonatal WT mice relative to E14.5 WT mice are activating one Organismal Growth and Development pathway (Sperm Motility, the four differentially expressed genes that lead to predicted activation and enrichment of this Canonical Pathway are *Ptk2B*, *Abhd3*, *Pla2G3 Prkcg*, which have diverse functions in several organismal growth, development, and metabolism-related Canonical Pathways, indicating that it is likely not sperm motility *per se* that is enriched, but a Canonical Pathways with overlapping genes) (72–75).

In 2wk WT mice relative to neonatal WT mice there are six activated Canonical Pathways. Three of these Canonical Pathways are in the Intracellular and Second Messenger Signaling category (α-Adrenergic Signaling, cAMP-mediated Signaling, and RhoA Signaling), two Canonical Pathways are in Phospholipid Biosynthesis (3-phosphoinositide Biosynthesis, and D-myo-inositol-5-phosphate metabolism), and one Canonical Pathway is the Nervous System Signaling category (Neuropathic Pain Signaling in Dorsal Horn Neurons). The only predicted and differentially expressed Upstream Regulator across the WT timeseries is *Eomes*, which is downregulated in this comparison and is involved in regulation of two of the pathways (3-phosphoinositide Biosynthesis, and D-myo-inositol-5-phosphate metabolism). Similar to the RdRP mice, there are no significantly activated or inhibited Canonical Pathways in 10wk WT mice relative to 2wk WT mice (Table V).

Furthermore, we used IPA Diseases and Biological Functions analyses to identify over- and under-represented Diseases and Biological Functions that differ between WT mice and RdRP mice across the time series and whether such functions are likely to be activated or inhibited (Table SIII). E14.5 RdRP mice relative to E10.5 RdRP mice are enriched for activated Diseases and Biological Functions that were largely related to neurological development and other neurological processes (*e.g.* Development of Neurons, Synaptic Transmission), and the growth, proliferation, and maintenance of cell function (*e.g.* Outgrowth of Cells, Organization of Cytoplasm), while Diseases and Biological Functions related to cancers/tumors (*e.g.* Secondary Tumor) and neurological abnormalities (*e.g.* Epilepsy) were inhibited. While most of the enriched GO terms are also related to development, four of the enriched GO terms are functions related to antigen processing and presentation, and immune cell (NK and T cell) cytotoxicity. All four of these GO terms are enriched because the genes *Raet1a*, *Raet1b*, *Raet1c*, *Raet1d*, *Raet1e* are downregulated in E14.5 RdRP mice relative to E10.5. However, FPKM values in RdRP and WT mice at E14.5

are nearly identical, and at E10.5 FPKM is only slightly higher in RdRP mice (FPKM 5.95 vs 4.86). This pattern suggests that these genes may decrease in expression slightly later or slower in RdRP mice, however, this remains to be tested. These genes are just below the significance thresholds for differential expression in the corresponding WT comparison. They may be interesting genes for future analyses as they are known to be expressed during embryogenesis, have been implicated in cellular response to exogenous dsRNA (only prior to E18) (76, 77) and *Raet1d*, and *Raet1e* are ISGs. Neonatal RdRP mice relative to E14.5 RdRP mice are activating one Biological Function related to organismal development (Transformation of Vertebrae) and, inhibiting one Biological Function related to tumors (Benign Lesion). There were no significantly enriched GO terms in this comparison.

For 2wk RdRP mice relative to neonatal RdRP mice, Biological Functions involved in immune system processes (*e.g.* Leukocyte Migration), and cell survival (*e.g.* Cell Viability) are activated, while Biological Functions related to nervous system degeneration (*e.g.* Degeneration of Neurons, Neurodegeneration of Axons), and mortality (*e.g.* Morbidity or Mortality, Organismal Death) are inhibited. Similarly, all seven enriched GO terms are involved in immune responses, in particular, innate immunity and cellular responses to interferon. Finally, 10wk RdRP mice relative to 2wk RdRP mice activating two related Biological Functions: Morbidity or Mortality, and Organismal Death. There were no significantly enriched GO terms in this comparison. Similar to the analyses described above, we only observe significant enrichment and activation of Diseases and Biological Functions related to the immune system in 2wk RdRP mice relative to neonatal RdRP mice, and that significant differences in activation/inhibition in these Canonical Pathways is not observed in 10wk RdRP mice relative to 2wk RdRP mice, suggests that the activation states are maintained over time (Table SIII).

We also identified enriched GO terms and IPA Diseases and Biological Functions that were enriched and showed significant evidence for activation or inhibition across the WT time series, that did not appear in the RdRP time series (Table SIII). E14.5 WT mice relative to E10.5 WT mice are activating Biological Functions related to transcription (*e.g.* Expression of RNA, Transcription of DNA), neurological processes (*e.g.* Plasticity of Synapse), and molecular transport (Transport of Metal), while inhibiting Biological Functions related to cellular movement (*e.g.* Movement/Migration of Vascular Endothelial Cells), and organismal development (*e.g.* Tensile Strength of Skin), and a transcription factor activity-related GO term is enriched. Neonatal WT mice relative to E14.5 WT mice are activating Biological Functions involved in lipid-related metabolic processes (*e.g.* Release of Lipid), organismal development (*e.g.* Development of Body Trunk), and cellular function and maintenance (*e.g.* Formation of Actin Filaments), and gene silencing by miRNAs is enriched. Neonatal WT mice are inhibiting one Biological Functions related to immune system processes, Apoptosis of T lymphocytes. While there are no inhibited Diseases and Biological Functions in 2wk WT mice relative to Neonatal WT mice, these mice are activating functions related to organismal development (*e.g.* Transformation of Vertebrae, Hypoplasia of Bone), lipid metabolism, cellular function and maintenance (*e.g.* Cellular Homeostasis), and neurological processes (Synaptic Depression). At this time point, development and DNA-binding-related GO terms are enriched. Unlike the RdRP mice, there are no enriched Diseases or Biological

Functions that are activated or inhibited in 10wk WT mice relative to 2wk WT mice (Table SIII).

Discussion

Previously, we demonstrated that adult RdRP mice exhibit dramatic induction of ISGs, are resistant to infection by diverse viruses, but are otherwise indistinguishable from WT mice. RdRP mice are able to maintain this reconfigured innate immune system without the negative consequence of autoimmunity or autoinflammation (27). Here, we demonstrate that the majority of this ISG induction occurs postnatally (Figs 2 **and** 3; Tables I **and** IV), and most noticeably in the 2wk and 10wk time points (Fig 2; Table I, Table SI). That there is little difference in gene expression patterns and pathways and functional enrichment in 10wk relative to 2wk RdRP further suggests that expression patterns are maintained thereafter (Fig 4; Table IV, Table SI). In other words, even though the RdRP transgene is expressed throughout embryonic development and into adulthood, RdRP mice do not mount a major innate immune response until after birth.

An important mechanistic finding emerged with regard to the maintenance of the constitutively elevated ISG expression in RdRP mice. Using an IFNAR neutralizing antibody, we show that the ISG profile can be reversed in adult RdRP mice and is not developmentally fixed at the level of ISG transcription (Fig 5). Second, these data indicate that ongoing, lifelong production of dsRNA by the RdRP to produce IFNs that signal through the type I interferon receptor is necessary for maintenance of the ISG response in RdRP mice. It might therefore be tunable to desired levels. Interestingly, while the MAR1-5A antibody treatment demonstrates that ISG induction is *ifnar*-dependent, we do not observe significant differential expression of Type I IFNs themselves. Consistent with this observation Painter et al. (27) also did not observe differential expression of Type I IFNs via microarray – suggesting that this pattern is technology-independent – even though crosses with *ifnar* −/− mice demonstrated that Type I IFN signaling is required for ISG activation.

Embryonic development requires proper, stepwise execution of many tightly regulated, interacting molecular pathways, including those related to innate immunity and inflammatory response. Although innate and adaptive immune cells are present during fetal development, they are considered to be poorly developed (34). This reflects the minimal exposure of the fetus to the microbial world and that both fetal self and maternal antigens must be reciprocally tolerated to ensure viability (78, 79). Furthermore, some molecular pathways involved in immune and inflammatory responses, such as NF-κB signaling, also play essential roles in development (80), and dysregulation of innate immunity can cause a wide range of deleterious pre- and postnatal outcomes.

RdRP-transgenic mice represent a unique model for the study of fetal responses to dsRNA PAMPs. While the RdRP transgene is expressed at every developmental stage that we sampled, a relatively small proportion of genes that are differentially expressed in RdRP mice relative to WT mice during the prenatal time points are known ISGs (Table I). Furthermore, most of the prenatal DEGs that overlapped with the Interferome database do

not represent canonical ISGs (e.g. ISGs that are dependent on the JAK-STAT pathway) (60–65) and/or have other known important functions in non-immune or inflammatory response-related processes. For example, among the 17 differentially expressed ISGs in E10.5 mice (Fig 2; Table SI), *Neurod2* and *Neurod6* are involved in nervous system development (81, 82) and *Hoxb2* and *Hoxb7* play important roles in the developmental patterning during embryonic development (83, 84). Likewise, among E14.5 differentially expressed ISGs, *Foxj2* is a transcriptional activator expressed in embryos (85), and *Kif1c* is also involved in neurological function (86). Whether genes such as these are being expressed primarily in neurological or developmental capacities *vs.* in immune-related functions remains unclear.

Despite only minor differential ISG induction in prenatal RdRP mice, several DEGs have established roles in immune response. For example, *Epcam* and *Krt18* are upregulated in E10.5 RdRP mice relative to E10.5 WT mice (Fig 2; Table SI). *Epcam* is involved in immune response to mucosal infection (87), whereas *Krt18* is involved in response to injury and infection (88). Interestingly, both of these genes are downregulated in E14.5 RdRP mice relative to E10.5 RdRP mice (Fig 4; Table SI), meaning that their induction is transient. Additionally, *Rps6ka4*, which is involved in p38 MAPK and TNF-mediated proinflammatory signaling (89) is downregulated in E14.5 RdRP mice relative to E14.5 WT mice and E10.5 RdRP mice (Figs 2 **and** 4; Table SI). Several other genes involved in immune and inflammatory response are also downregulated in E14.5 RdRP mice relative to E10.5 RdRP mice such as *Ermap* (an adhesion/receptor molecule for erythroid cells) (90), *Hlx* (required for the maturation of Th1 cells and Th1-specific gene expression) (91), and *Itga9* (involved in neutrophil chemotaxis and wound healing) (Fig 4; Table SI) (92). These results suggest that there may be an increased bias against inflammation in E14.5 RdRP mice relative to E10.5 RdRP mice and/or that type I interferon independent immune pathways may be active in prenatal development, such as RhoA Signaling (Tables II **and** V), which is suggested to be involved in IFN-γ-related immune regulation. Moreover, both the pairwise and time series gene expression comparisons revealed early developmental RdRP-mediated changes in prenatal Canonical Pathways, Biological Functions, and GO enrichment. For example, the inhibition of Biological Functions related to morbidity and mortality, and developmental abnormalities (Tables III **and** SIII). We also observed putative patterns of repression in RdRP mice compared to WT mice over the time series. For example, *Ubn2* is expressed at similar levels in RdRP and WT mice at E10.5. In WT mice *Ubn2* then rapidly increases in expression and is maintained at relatively high levels until decreasing again between 2wk and 10wk time points, whereas relatively lower expression of this gene in maintained throughout the life of RdRP mice. However, potential associations between chronic RdRP mediated PAMP expression and gene expression patterns of embryonic mice, alongside potential contributions of maternal RdRP expression and maternal ISG induction on changes in the early embryo remain to be characterized. Future exploration of genes that appear to be repressed in RdRP mice during prenatal development compared to WT mice could help disentangle the lack of developmental abnormalities or embryonic lethality in RdRP mice.

Birth results in a sudden transition from the shielded and largely sterile uterine environment to a world that teems with microbes. Placental oxygenation is replaced by autonomous

respiration and the gut and integument are rapidly colonized by large numbers of microorganisms. Immediately after birth, the neonatal immune system is highly similar to the fetal immune system (78, 93), is biased against inflammatory responses (42), and leaves neonates vulnerable to infection (78, 94). The period during and shortly after birth is characterized by colonization of the neonate by pathogenic and non-pathogenic microbes leading to altered immune cell phenotype and function and immune activation, processes which need to be balanced against the potential for autoimmunity and harmful inflammation (78, 95, 96). In humans, for example, the IL-6-mediated acute phase response is thought to help protect neonates from infection while limiting excessive inflammation, is highly expressed after birth, and can exceed the expression level of adults (42, 97).

Neonatal RdRP mice had similarly suppressed induction of type I interferon responses as embryonic mice; however, the pattern of DEGs began to shift by this stage of development. A number of interferon pathway regulators were differentially expressed between RdRP and WT mice in neonates. For example, *Pde12*, which is a negative regulator of IFN-induced antiviral pathways and cellular response to dsRNA is downregulated (98). Further, *Rtp4* is involved in both olfactory reception (99) and defense response to viruses (100). *Scgb1a1*, a negative regulator of IFN-γ, has been implicated in anti-inflammation, inhibition of phospholipase A2 and the sequestering of hydrophobic ligands (101, 102). However, our previous work has shown that knock out of the IFN-γ receptor (*Ifngr1*) had no effect on ISG profile of RdRP mice (27). Both are upregulated in neonatal RdRP mice relative to neonatal WT mice. In addition, *Scgb1* is also strongly upregulated in RdRP mice at E10.5 and E14.5. Similarly, *Rps6ka4*, which was downregulated at E14.5, is upregulated in neonatal RdRP mice relative to E14.5 RdRP mice (Fig 4; Table SI). While most of the Biological Functions that were activated in neonatal WT mice relative to E14.5 WT mice are involved in metabolic processes and development, they are also inhibiting Apoptosis of T lymphocytes, likely influenced by the > 100x downregulation of *Cd27* in neonatal WT mice relative to E14.5 WT mice. Inhibition of this Biological Function could be indicative of the normal expansion and maturation of this cell type that occurs shortly after birth (103). That we do not see similar enriched Biological Functions in RdRP mice at this time point may suggest differences in the timing of immune system developmental processes between WT and RdRP mice. In sum, these results are suggestive of the beginning of an innate immune and inflammatory response to PAMP expression in neonatal mice.

In summary, we have shown that transgenic mice expressing a picornavirus RNA-dependent RNA polymerase exhibit substantial induction of numerous ISGs. Importantly, we used RNA-seq to demonstrate that, while there are differences in gene expression between WT and RdRP mice during embryogenesis, the massive ISG induction in RdRP mice does not occur until after the neonatal time point. Following initial ISG induction, this gene expression profile is then maintained throughout adulthood without triggering harmful autoimmune or autoinflammatory problems. We also found that Canonical Pathways, Biological Functions, and enriched GO terms associated with immune system function and most notably, interferon signaling, are only enriched and/or activated in the two- and ten-week-old RdRP mice. It is at these same two time points that we observed inhibition of Biological Functions associated with viral infection and replication. Future work, geared towards understanding potential developmental and/or neurological differences between WT

and RdRP mice during embryogenesis, or potential fetal mechanisms or maternal effects dampening innate immune response to RdRP PAMPs *in utero* will be of great interest. Remarkably, with this system, we are able to demonstrate that a substantial MDA5, MAVS, and IFNAR-dependent reconfiguration of the innate immune system can be broadly tolerated and compatible with robust mammalian health. The model has potential for understanding how to prevent or treat autoimmune diseases and has therapeutic implications for augmenting post-natal innate immunity to viral infection.

Supplementary Material

Refer to Web version on PubMed Central for supplementary material.

Acknowledgements

We thank Aaron Massey for assistance with dissections.

This work was funded by an NIH Avant-Garde Grant (NIH 1DP1DA043915) and a Tietze Foundation Grant to E.M. Poeschla

References

1. Chan YK, and Gack MU. 2016 Viral evasion of intracellular DNA and RNA sensing. Nature reviews. Microbiology 14: 360–373. [PubMed: 27174148]
2. Goubau D, Deddouche S, and Reis e Sousa C. 2013 Cytosolic sensing of viruses. Immunity 38: 855–869. [PubMed: 23706667]
3. Lassig C, and Hopfner KP. 2017 Discrimination of cytosolic self and non-self RNA by RIG-I-like receptors. The Journal of biological chemistry 292: 9000–9009. [PubMed: 28411239]
4. Takahasi K, Yoneyama M, Nishihori T, Hirai R, Kumeta H, Narita R, Gale M Jr., Inagaki F, and Fujita T. 2008 Nonself RNA-sensing mechanism of RIG-I helicase and activation of antiviral immune responses. Molecular cell 29: 428–440. [PubMed: 18242112]
5. Roers A, Hiller B, and Hornung V. 2016 Recognition of Endogenous Nucleic Acids by the Innate Immune System. Immunity 44: 739–754. [PubMed: 27096317]
6. Kato H, Takeuchi O, Sato S, Yoneyama M, Yamamoto M, Matsui K, Uematsu S, Jung A, Kawai T, Ishii KJ, Yamaguchi O, Otsu K, Tsujimura T, Koh CS, Reis e Sousa C, Matsuura Y, Fujita T, and Akira S. 2006 Differential roles of MDA5 and RIG-I helicases in the recognition of RNA viruses. Nature 441: 101–105. [PubMed: 16625202]
7. Gitlin L, Barchet W, Gilfillan S, Cella M, Beutler B, Flavell RA, Diamond MS, and Colonna M. 2006 Essential role of mda-5 in type I IFN responses to polyriboinosinic:polyribocytidylic acid and encephalomyocarditis picornavirus. Proceedings of the National Academy of Sciences of the United States of America 103: 8459–8464. [PubMed: 16714379]
8. Kato H, Sato S, Yoneyama M, Yamamoto M, Uematsu S, Matsui K, Tsujimura T, Takeda K, Fujita T, Takeuchi O, and Akira S. 2005 Cell type-specific involvement of RIG-I in antiviral response. Immunity 23: 19–28. [PubMed: 16039576]
9. Hornung V, Ellegast J, Kim S, Brzozka K, Jung A, Kato H, Poeck H, Akira S, Conzelmann KK, Schlee M, Endres S, and Hartmann G. 2006 5′-Triphosphate RNA is the ligand for RIG-I. Science 314: 994–997. [PubMed: 17038590]
10. Kawai T, Takahashi K, Sato S, Coban C, Kumar H, Kato H, Ishii KJ, Takeuchi O, and Akira S. 2005 IPS-1, an adaptor triggering RIG-I- and Mda5-mediated type I interferon induction. Nature immunology 6: 981–988. [PubMed: 16127453]
11. Meylan E, Curran J, Hofmann K, Moradpour D, Binder M, Bartenschlager R, and Tschopp J. 2005 Cardif is an adaptor protein in the RIG-I antiviral pathway and is targeted by hepatitis C virus. Nature 437: 1167–1172. [PubMed: 16177806]

12. Seth RB, Sun L, Ea CK, and Chen ZJ. 2005 Identification and characterization of MAVS, a mitochondrial antiviral signaling protein that activates NF-kappaB and IRF 3. Cell 122: 669–682. [PubMed: 16125763]

13. Cardoso-Moreira M, Halbert J, Valloton D, Velten B, Chen C, Shao Y, Liechti A, Ascenção K, Rummel C, Ovchinnikova S, Mazin PV, Xenarios I, Harshman K, Mort M, Cooper DN, Sandi C, Soares MJ, Ferreira PG, Afonso S, Carneiro M, Turner JMA, VandeBerg JL, Fallahshahroudi A, Jensen P, Behr R, Lisgo S, Lindsay S, Khaitovich P, Huber W, Baker J, Anders S, Zhang YE, and Kaessmann H. 2019 Gene expression across mammalian organ development. Nature 571: 505–509. [PubMed: 31243369]

14. Crow YJ, and Manel N. 2015 Aicardi-Goutieres syndrome and the type I interferonopathies. Nature reviews. Immunology 15: 429–440.

15. Ronnblom L 2016 The importance of the type I interferon system in autoimmunity. Clin Exp Rheumatol 34: 21–24. [PubMed: 27586799]

16. Crow YJ, Hayward BE, Parmar R, Robins P, Leitch A, Ali M, Black DN, van Bokhoven H, Brunner HG, Hamel BC, Corry PC, Cowan FM, Frints SG, Klepper J, Livingston JH, Lynch SA, Massey RF, Meritet JF, Michaud JL, Ponsot G, Voit T, Lebon P, Bonthron DT, Jackson AP, Barnes DE, and Lindahl T. 2006 Mutations in the gene encoding the 3′–5′ DNA exonuclease TREX1 cause Aicardi-Goutieres syndrome at the AGS1 locus. Nature genetics 38: 917–920. [PubMed: 16845398]

17. Funabiki M, Kato H, Miyachi Y, Toki H, Motegi H, Inoue M, Minowa O, Yoshida A, Deguchi K, Sato H, Ito S, Shiroishi T, Takeyasu K, Noda T, and Fujita T. 2014 Autoimmune Disorders Associated with Gain of Function of the Intracellular Sensor MDA5. Immunity 40: 199–212. [PubMed: 24530055]

18. Gorman JA, Hundhausen C, Errett JS, Stone AE, Allenspach EJ, Ge Y, Arkatkar T, Clough C, Dai X, Khim S, Pestal K, Liggitt D, Cerosaletti K, Stetson DB, James RG, Oukka M, Concannon P, Gale M Jr., Buckner JH, and Rawlings DJ. 2017 The A946T variant of the RNA sensor IFIH1 mediates an interferon program that limits viral infection but increases the risk for autoimmunity. Nature immunology 18: 744–752. [PubMed: 28553952]

19. Rice GI, del Toro Duany Y, Jenkinson EM, Forte GM, Anderson BH, Ariaudo G, Bader-Meunier B, Baildam EM, Battini R, Beresford MW, Casarano M, Chouchane M, Cimaz R, Collins AE, Cordeiro NJ, Dale RC, Davidson JE, De Waele L, Desguerre I, Faivre L, Fazzi E, Isidor B, Lagae L, Latchman AR, Lebon P, Li C, Livingston JH, Lourenco CM, Mancardi MM, Masurel-Paulet A, McInnes IB, Menezes MP, Mignot C, O'Sullivan J, Orcesi S, Picco PP, Riva E, Robinson RA, Rodriguez D, Salvatici E, Scott C, Szybowska M, Tolmie JL, Vanderver A, Vanhulle C, Vieira JP, Webb K, Whitney RN, Williams SG, Wolfe LA, Zuberi SM, Hur S, and Crow YJ. 2014 Gain-of-function mutations in MDA5 (IFIH1) cause a spectrum of human disease phenotypes associated with upregulated type I interferon signaling. Nature genetics 46: 503–509. [PubMed: 24686847]

20. Rice G, Newman WG, Dean J, Patrick T, Parmar R, Flintoff K, Robins P, Harvey S, Hollis T, O'Hara A, Herrick AL, Bowden AP, Perrino FW, Lindahl T, Barnes DE, and Crow YJ. 2007 Heterozygous mutations in TREX1 cause familial chilblain lupus and dominant Aicardi-Goutieres syndrome. American journal of human genetics 80: 811–815. [PubMed: 17357087]

21. Lee-Kirsch MA, Gong M, Chowdhury D, Senenko L, Engel K, Lee YA, de Silva U, Bailey SL, Witte T, Vyse TJ, Kere J, Pfeiffer C, Harvey S, Wong A, Koskenmies S, Hummel O, Rohde K, Schmidt RE, Dominiczak AF, Gahr M, Hollis T, Perrino FW, Lieberman J, and Hubner N. 2007 Mutations in the gene encoding the 3′–5′ DNA exonuclease TREX1 are associated with systemic lupus erythematosus. Nature genetics 39: 1065–1067. [PubMed: 17660818]

22. Stetson DB, Ko JS, Heidmann T, and Medzhitov R. 2008 Trex1 prevents cell-intrinsic initiation of autoimmunity. Cell 134: 587–598. [PubMed: 18724932]

23. Rice GI, Rodero MP, and Crow YJ. 2015 Human disease phenotypes associated with mutations in TREX1. Journal of clinical immunology 35: 235–243. [PubMed: 25731743]

24. Yan N, Cherepanov P, Daigle JE, Engelman A, and Lieberman J. 2009 The SET complex acts as a barrier to autointegration of HIV-1. PLoS pathogens 5: e1000327. [PubMed: 19266025]

25. Wheeler LA, Trifonova RT, Vrbanac V, Barteneva NS, Liu X, Bollman B, Onofrey L, Mulik S, Ranjbar S, Luster AD, Tager AM, and Lieberman J. 2016 TREX1 Knockdown Induces an

Interferon Response to HIV that Delays Viral Infection in Humanized Mice. Cell reports 15: 1715–1727. [PubMed: 27184854]

26. Kumar S, Morrison J, Dingli D, and Poeschla E. 2016 HIV-1 induction of interferon-stimulated genes depends strongly on intracellular levels of TREX1 and sensing of incomplete reverse transcription products. Submitted.
27. Painter MM, Morrison JH, Zoecklein LJ, Rinkoski TA, Watzlawik JO, Papke LM, Warrington AE, Bieber AJ, Matchett WE, Turkowski KL, Poeschla EM, and Rodriguez M. 2015 Antiviral Protection via RdRP-Mediated Stable Activation of Innate Immunity. PLoS pathogens 11: e1005311. [PubMed: 26633895]
28. den Boon JA, Diaz A, and Ahlquist P. 2010 Cytoplasmic viral replication complexes. Cell host & microbe 8: 77–85. [PubMed: 20638644]
29. Paul D, and Bartenschlager R. 2013 Architecture and biogenesis of plus-strand RNA virus replication factories. World journal of virology 2: 32–48. [PubMed: 24175228]
30. Melia CE, Peddie CJ, de Jong AWM, Snijder EJ, Collinson LM, Koster AJ, van der Schaar HM, van Kuppeveld FJM, and Barcena M. 2019 Origins of Enterovirus Replication Organelles Established by Whole-Cell Electron Microscopy. mBio 10.
31. Laufman O, Perrino J, and Andino R. 2019 Viral Generated Inter-Organelle Contacts Redirect Lipid Flux for Genome Replication. Cell 178: 275–289 e216. [PubMed: 31204099]
32. Kerkvliet J, Zoecklein L, Papke L, Denic A, Bieber AJ, Pease LR, David CS, and Rodriguez M. 2009 Transgenic expression of the 3D polymerase inhibits Theiler's virus infection and demyelination. Journal of virology 83: 12279–12289. [PubMed: 19759133]
33. Kerkvliet J, Papke L, and Rodriguez M. 2011 Antiviral effects of a transgenic RNA-dependent RNA polymerase. Journal of virology 85: 621–625. [PubMed: 20962089]
34. Yockey LJ, and Iwasaki A. 2018 Interferons and Proinflammatory Cytokines in Pregnancy and Fetal Development. Immunity 49: 397–412. [PubMed: 30231982]
35. Yockey LJ, Jurado KA, Arora N, Millet A, Rakib T, Milano KM, Hastings AK, Fikrig E, Kong Y, Horvath TL, Weatherbee S, Kliman HJ, Coyne CB, and Iwasaki A. 2018 Type I interferons instigate fetal demise after Zika virus infection. Sci Immunol 3.
36. Sullivan KD, Lewis HC, Hill AA, Pandey A, Jackson LP, Cabral JM, Smith KP, Liggett LA, Gomez EB, Galbraith MD, DeGregori J, and Espinosa JM. 2016 Trisomy 21 consistently activates the interferon response. eLife 5.
37. Thaxton JE, Nevers T, Lippe EO, Blois SM, Saito S, and Sharma S. 2013 NKG2D blockade inhibits poly(I:C)-triggered fetal loss in wild type but not in IL-10−/− mice. J Immunol 190: 3639–3647. [PubMed: 23455498]
38. Mader SL, Libal NL, Pritchett-Corning K, Yang R, and Murphy SJ. 2009 Refining timed pregnancies in two strains of genetically engineered mice. Lab Anim (NY) 38: 305–310. [PubMed: 19701181]
39. Hill M Embryology: Mouse Timeline Detailed https://embryology.med.unsw.edu.au/embryology/index.php/Mouse_Timeline_Detailed [cited 2018 21 September].
40. Harju K, Glumoff V, and Hallman M. 2001 Ontogeny of Toll-like receptors Tlr2 and Tlr4 in mice. Pediatr Res 49: 81–83. [PubMed: 11134496]
41. Yoshida H, Okabe Y, Kawane K, Fukuyama H, and Nagata S. 2005 Lethal anemia caused by interferon-beta produced in mouse embryos carrying undigested DNA. Nature immunology 6: 49–56. [PubMed: 15568025]
42. Levy O 2007 Innate immunity of the newborn: basic mechanisms and clinical correlates. Nature reviews. Immunology 7: 379–390.
43. Andrews S FASTQC: A quality control tool for high throughput sequence data. FASTQC. 0.11.5 ed. http://www.bioinformatics.babraham.ac.uk?/projects/fastqc/2010.
44. Gordon A, and Hannon G. Fastx-toolkit. FASTQ/A short-read pre-processing tools. Fastx-toolkit. 0.0.13 ed. http://hannonlabcshledu/fastx_toolkit/2010.
45. Dobin A, Davis CA, Schlesinger F, Drenkow J, Zaleski C, Jha S, Batut P, Chaisson M, and Gingeras TR. 2013 STAR: ultrafast universal RNA-seq aligner. Bioinformatics 29: 15–21. [PubMed: 23104886]

46. Li H, Handsaker B, Wysoker A, Fennell T, Ruan J, Homer N, Marth G, Abecasis G, Durbin R, and Genome S Project Data Processing. 2009. The Sequence Alignment/Map format and SAMtools. Bioinformatics 25: 2078–2079. [PubMed: 19505943]
47. Picard Tools. http://picard.sourceforge.net: Broad Institute.
48. Trapnell C, Williams BA, Pertea G, Mortazavi A, Kwan G, van Baren MJ, Salzberg SL, Wold BJ, and Pachter L. 2010 Transcript assembly and quantification by RNA-Seq reveals unannotated transcripts and isoform switching during cell differentiation. Nature biotechnology 28: 511–515.
49. Trapnell C, Roberts A, Goff L, Pertea G, Kim D, Kelley DR, Pimentel H, Salzberg SL, Rinn JL, and Pachter L. 2012 Differential gene and transcript expression analysis of RNA-seq experiments with TopHat and Cufflinks. Nature protocols 7: 562–578. [PubMed: 22383036]
50. Conesa A, Madrigal P, Tarazona S, Gomez-Cabrero D, Cervera A, McPherson A, Szczesniak MW, Gaffney DJ, Elo LL, Zhang X, and Mortazavi A. 2016 A survey of best practices for RNA-seq data analysis. Genome Biol 17: 13. [PubMed: 26813401]
51. Goff L, Trapnell C, and Kelley DR. CummeRbund: Analysis, exploration, manipulation, and visualization of Cufflinks high-throughput sequencing data. 3.4.2 ed2013.
52. Collaborative data science Publisher: Plotly Technologies Inc.
53. Rusinova I, Forster S, Yu S, Kannan A, Masse M, Cumming H, Chapman R, and Hertzog PJ. 2013 Interferome v2.0: an updated database of annotated interferon-regulated genes. Nucleic acids research 41: D1040–1046. [PubMed: 23203888]
54. _. Ingenuity Pathway Analysis. https://www.qiagenbioinformatics.com/products/ingenuity-pathway-analysis.: QIAGEN Inc
55. Ashburner M, Ball CA, Blake JA, Botstein D, Butler H, Cherry JM, Davis AP, Dolinski K, Dwight SS, Eppig JT, Harris MA, Hill DP, Issel-Tarver L, Kasarskis A, Lewis S, Matese JC, Richardson JE, Ringwald M, Rubin GM, and Sherlock G. 2000 Gene ontology: tool for the unification of biology. The Gene Ontology Consortium. Nature genetics 25: 25–29. [PubMed: 10802651]
56. The Gene Ontology C 2019 The Gene Ontology Resource: 20 years and still GOing strong. Nucleic acids research 47: D330–D338. [PubMed: 30395331]
57. Huang da W, Sherman BT, and Lempicki RA. 2009 Bioinformatics enrichment tools: paths toward the comprehensive functional analysis of large gene lists. Nucleic acids research 37: 1–13. [PubMed: 19033363]
58. Huang da W, Sherman BT, and Lempicki RA. 2009 Systematic and integrative analysis of large gene lists using DAVID bioinformatics resources. Nature protocols 4: 44–57. [PubMed: 19131956]
59. Mader SL, Libal NL, Pritchett-Corning K, Yang R, and Murphy SJ. 2009 Refining timed pregnancies in two strains of genetically engineered mice. Lab Animal 38: 305–310. [PubMed: 19701181]
60. Cho H, Proll SC, Szretter KJ, Katze MG, Gale M Jr., and Diamond MS. 2013 Differential innate immune response programs in neuronal subtypes determine susceptibility to infection in the brain by positive-stranded RNA viruses. Nature medicine 19: 458–464.
61. de Veer MJ, Holko M, Frevel M, Walker E, Der S, Paranjape JM, Silverman RH, and Williams BR. 2001 Functional classification of interferon-stimulated genes identified using microarrays. Journal of leukocyte biology 69: 912–920. [PubMed: 11404376]
62. Itsui Y, Sakamoto N, Kurosaki M, Kanazawa N, Tanabe Y, Koyama T, Takeda Y, Nakagawa M, Kakinuma S, Sekine Y, Maekawa S, Enomoto N, and Watanabe M. 2006 Expressional screening of interferon-stimulated genes for antiviral activity against hepatitis C virus replication. J Viral Hepat 13: 690–700. [PubMed: 16970601]
63. Jiang D, Weidner JM, Qing M, Pan XB, Guo H, Xu C, Zhang X, Birk A, Chang J, Shi PY, Block TM, and Guo JT. 2010 Identification of five interferon-induced cellular proteins that inhibit west nile virus and dengue virus infections. Journal of virology 84: 8332–8341. [PubMed: 20534863]
64. Schneider WM, Chevillotte MD, and Rice CM. 2014 Interferon-stimulated genes: a complex web of host defenses. Annual review of immunology 32: 513–545.
65. Schoggins JW, MacDuff DA, Imanaka N, Gainey MD, Shrestha B, Eitson JL, Mar KB, Richardson RB, Ratushny AV, Litvak V, Dabelic R, Manicassamy B, Aitchison JD, Aderem A, Elliott RM, Garcia-Sastre A, Racaniello V, Snijder EJ, Yokoyama WM, Diamond MS, Virgin HW, and Rice

CM. 2014 Pan-viral specificity of IFN-induced genes reveals new roles for cGAS in innate immunity. Nature 505: 691–695. [PubMed: 24284630]

66. Tamura T, Yanai H, Savitsky D, and Taniguchi T. 2008 The IRF family transcription factors in immunity and oncogenesis. Annual review of immunology 26: 535–584.
67. Bhagwat SP, Gigliotti F, Wang J, Wang Z, Notter RH, Murphy PS, Rivera-Escalera F, Malone J, Jordan MB, Elliott MR, and Wright TW. 2018 Intrinsic Programming of Alveolar Macrophages for Protective Antifungal Innate Immunity Against Pneumocystis Infection. Front Immunol 9: 2131. [PubMed: 30283457]
68. Van Aelst L, and D'Souza-Schorey C. 1997 Rho GTPases and signaling networks. Genes Dev 11: 2295–2322. [PubMed: 9308960]
69. Bokoch GM 2005 Regulation of innate immunity by Rho GTPases. Trends Cell Biol 15: 163–171. [PubMed: 15752980]
70. Bros M, Haas K, Moll L, and Grabbe S. 2019 RhoA as a Key Regulator of Innate and Adaptive Immunity. Cells 8.
71. Chiba H, Kojima T, Osanai M, and Sawada N. 2006 The significance of interferon-gamma-triggered internalization of tight-junction proteins in inflammatory bowel disease. Sci STKE 2006: pe1. [PubMed: 16391178]
72. Beverdam A, Svingen T, Bagheri-Fam S, McClive P, Sinclair AH, Harley VR, and Koopman P. 2010 Protein tyrosine kinase 2 beta (PTK2B), but not focal adhesion kinase (FAK), is expressed in a sexually dimorphic pattern in developing mouse gonads. Developmental dynamics : an official publication of the American Association of Anatomists 239: 2735–2741. [PubMed: 20737507]
73. Lord CC, Thomas G, and Brown JM. 2013 Mammalian alpha beta hydrolase domain (ABHD) proteins: Lipid metabolizing enzymes at the interface of cell signaling and energy metabolism. Biochim Biophys Acta 1831: 792–802. [PubMed: 23328280]
74. Shimobayashi E, and Kapfhammer JP. 2018 Calcium Signaling, PKC Gamma, IP3R1 and CAR8 Link Spinocerebellar Ataxias and Purkinje Cell Dendritic Development. Curr Neuropharmacol 16: 151–159. [PubMed: 28554312]
75. Starkl P, Marichal T, and Galli SJ. 2013 PLA2G3 promotes mast cell maturation and function. Nature immunology 14: 527–529. [PubMed: 23685814]
76. Cerwenka A, Bakker AB, McClanahan T, Wagner J, Wu J, Phillips JH, and Lanier LL. 2000 Retinoic acid early inducible genes define a ligand family for the activating NKG2D receptor in mice. Immunity 12: 721–727. [PubMed: 10894171]
77. Zou Z, Nomura M, Takihara Y, Yasunaga T, and Shimada K. 1996 Isolation and characterization of retinoic acid-inducible cDNA clones in F9 cells: a novel cDNA family encodes cell surface proteins sharing partial homology with MHC class I molecules. J Biochem 119: 319–328. [PubMed: 8882725]
78. Gollwitzer ES, and Marsland BJ. 2015 Impact of Early-Life Exposures on Immune Maturation and Susceptibility to Disease. Trends in immunology 36: 684–696. [PubMed: 26497259]
79. Mold JE, Michaelsson J, Burt TD, Muench MO, Beckerman KP, Busch MP, Lee TH, Nixon DF, and McCune JM. 2008 Maternal alloantigens promote the development of tolerogenic fetal regulatory T cells in utero. Science 322: 1562–1565. [PubMed: 19056990]
80. Xu C, Wu X, Zhang X, Xie Q, Fan C, and Zhang H. 2018 Embryonic Lethality and Host Immunity of RelA-Deficient Mice Are Mediated by Both Apoptosis and Necroptosis. J Immunol 200: 271–285. [PubMed: 29167229]
81. Olson JM, Asakura A, Snider L, Hawkes R, Strand A, Stoeck J, Hallahan A, Pritchard J, and Tapscott SJ. 2001 NeuroD2 is necessary for development and survival of central nervous system neurons. Developmental biology 234: 174–187. [PubMed: 11356028]
82. Wu SX, Goebbels S, Nakamura K, Nakamura K, Kometani K, Minato N, Kaneko T, Nave KA, and Tamamaki N. 2005 Pyramidal neurons of upper cortical layers generated by NEX-positive progenitor cells in the subventricular zone. Proceedings of the National Academy of Sciences of the United States of America 102: 17172–17177. [PubMed: 16284248]
83. Sham MH, Vesque C, Nonchev S, Marshall H, Frain M, Gupta RD, Whiting J, Wilkinson D, Charnay P, and Krumlauf R. 1993 The zinc finger gene Krox20 regulates HoxB2 (Hox2.8) during hindbrain segmentation. Cell 72: 183–196. [PubMed: 8093858]

84. Vogels R, Charite J, de Graaff W, and Deschamps J. 1993 Proximal cis-acting elements cooperate to set Hoxb-7 (Hox-2.3) expression boundaries in transgenic mice. Development 118: 71–82. [PubMed: 8104144]
85. Granadino B, Arias-de-la-Fuente C, Perez-Sanchez C, Parraga M, Lopez-Fernandez LA, del Mazo J, and Rey-Campos J. 2000 Fhx (Foxj2) expression is activated during spermatogenesis and very early in embryonic development. Mechanisms of development 97: 157–160. [PubMed: 11025217]
86. Dor T, Cinnamon Y, Raymond L, Shaag A, Bouslam N, Bouhouche A, Gaussen M, Meyer V, Durr A, Brice A, Benomar A, Stevanin G, Schuelke M, and Edvardson S. 2014 KIF1C mutations in two families with hereditary spastic paraparesis and cerebellar dysfunction. J Med Genet 51: 137–142. [PubMed: 24319291]
87. Trzpis M, McLaughlin PM, de Leij LM, and Harmsen MC. 2007 Epithelial cell adhesion molecule: more than a carcinoma marker and adhesion molecule. The American journal of pathology 171: 386–395. [PubMed: 17600130]
88. Strnad P, Lienau TC, Tao GZ, Lazzeroni LC, Stickel F, Schuppan D, and Omary MB. 2006 Keratin variants associate with progression of fibrosis during chronic hepatitis C infection. Hepatology 43: 1354–1363. [PubMed: 16729313]
89. Coulthard LR, Taylor JC, Eyre S, Biologics G in Rheumatoid Arthritis, Genomics, Robinson JI, Wilson AG, Isaacs JD, Hyrich K, Emery P, Barton A, Barrett JH, Morgan AW, and McDermott MF. 2011 Genetic variants within the MAP kinase signalling network and anti-TNF treatment response in rheumatoid arthritis patients. Ann Rheum Dis 70: 98–103. [PubMed: 20805296]
90. Ye TZ, Gordon CT, Lai YH, Fujiwara Y, Peters LL, Perkins AC, and Chui DH. 2000 Ermap, a gene coding for a novel erythroid specific adhesion/receptor membrane protein. Gene 242: 337–345. [PubMed: 10721728]
91. Mullen AC, Hutchins AS, High FA, Lee HW, Sykes KJ, Chodosh LA, and Reiner SL. 2002 Hlx is induced by and genetically interacts with T-bet to promote heritable T(H)1 gene induction. Nature immunology 3: 652–658. [PubMed: 12055627]
92. Taooka Y, Chen J, Yednock T, and Sheppard D. 1999 The integrin alpha9beta1 mediates adhesion to activated endothelial cells and transendothelial neutrophil migration through interaction with vascular cell adhesion molecule-1. The Journal of cell biology 145: 413–420. [PubMed: 10209034]
93. Adkins B, Leclerc C, and Marshall-Clarke S. 2004 Neonatal adaptive immunity comes of age. Nature reviews. Immunology 4: 553–564.
94. Wilson CB, Westall J, Johnston L, Lewis DB, Dower SK, and Alpert AR. 1986 Decreased production of interferon-gamma by human neonatal cells. Intrinsic and regulatory deficiencies. The Journal of clinical investigation 77: 860–867. [PubMed: 3081575]
95. Dowling DJ, and Levy O. 2014 Ontogeny of early life immunity. Trends in immunology 35: 299–310. [PubMed: 24880460]
96. Weinberger B, Vetrano AM, Syed K, Murthy S, Hanna N, Laskin JD, and Laskin DL. 2007 Influence of labor on neonatal neutrophil apoptosis, and inflammatory activity. Pediatr Res 61: 572–577. [PubMed: 17413861]
97. Angelone DF, Wessels MR, Coughlin M, Suter EE, Valentini P, Kalish LA, and Levy O. 2006 Innate immunity of the human newborn is polarized toward a high ratio of IL-6/TNF-alpha production in vitro and in vivo. Pediatr Res 60: 205–209. [PubMed: 16864705]
98. Wood ER, Bledsoe R, Chai J, Daka P, Deng H, Ding Y, Harris-Gurley S, Kryn LH, Nartey E, Nichols J, Nolte RT, Prabhu N, Rise C, Sheahan T, Shotwell JB, Smith D, Tai V, Taylor JD, Tomberlin G, Wang L, Wisely B, You S, Xia B, and Dickson H. 2015 The Role of Phosphodiesterase 12 (PDE12) as a Negative Regulator of the Innate Immune Response and the Discovery of Antiviral Inhibitors. The Journal of biological chemistry 290: 19681–19696. [PubMed: 26055709]
99. Saito H, Kubota M, Roberts RW, Chi Q, and Matsunami H. 2004 RTP family members induce functional expression of mammalian odorant receptors. Cell 119: 679–691. [PubMed: 15550249]
100. Schoggins JW, and Rice CM. 2011 Interferon-stimulated genes and their antiviral effector functions. Curr Opin Virol 1: 519–525. [PubMed: 22328912]

101. Cabre F, Moreno JJ, Carabaza A, Ortega E, Mauleon D, and Carganico G. 1992 Antiflammins. Anti-inflammatory activity and effect on human phospholipase A2. Biochem Pharmacol 44: 519–525. [PubMed: 1387313]

102. Tian B, Yang J, Zhao Y, Ivanciuc T, Sun H, Wakamiya M, Garofalo RP, and Brasier AR. 2018 Central Role of the NF-kappaB Pathway in the Scgb1a1-Expressing Epithelium in Mediating Respiratory Syncytial Virus-Induced Airway Inflammation. Journal of virology 92.

103. Nouatin O, Gbedande K, Ibitokou S, Vianou B, Houngbegnon P, Ezinmegnon S, Borgella S, Akplogan C, Cottrell G, Varani S, Massougbodji A, Moutairou K, Troye-Blomberg M, Deloron P, Luty AJ, and Fievet N. 2015 Infants' Peripheral Blood Lymphocyte Composition Reflects Both Maternal and Post-Natal Infection with Plasmodium falciparum. PloS one 10: e0139606. [PubMed: 26580401]

Key points

- The augmented ISG profile of RdRP mice develops largely postnatally
- Elevated ISG expression is then maintained through adulthood
- The ISG signature in adults requires persistent type I interferon signaling

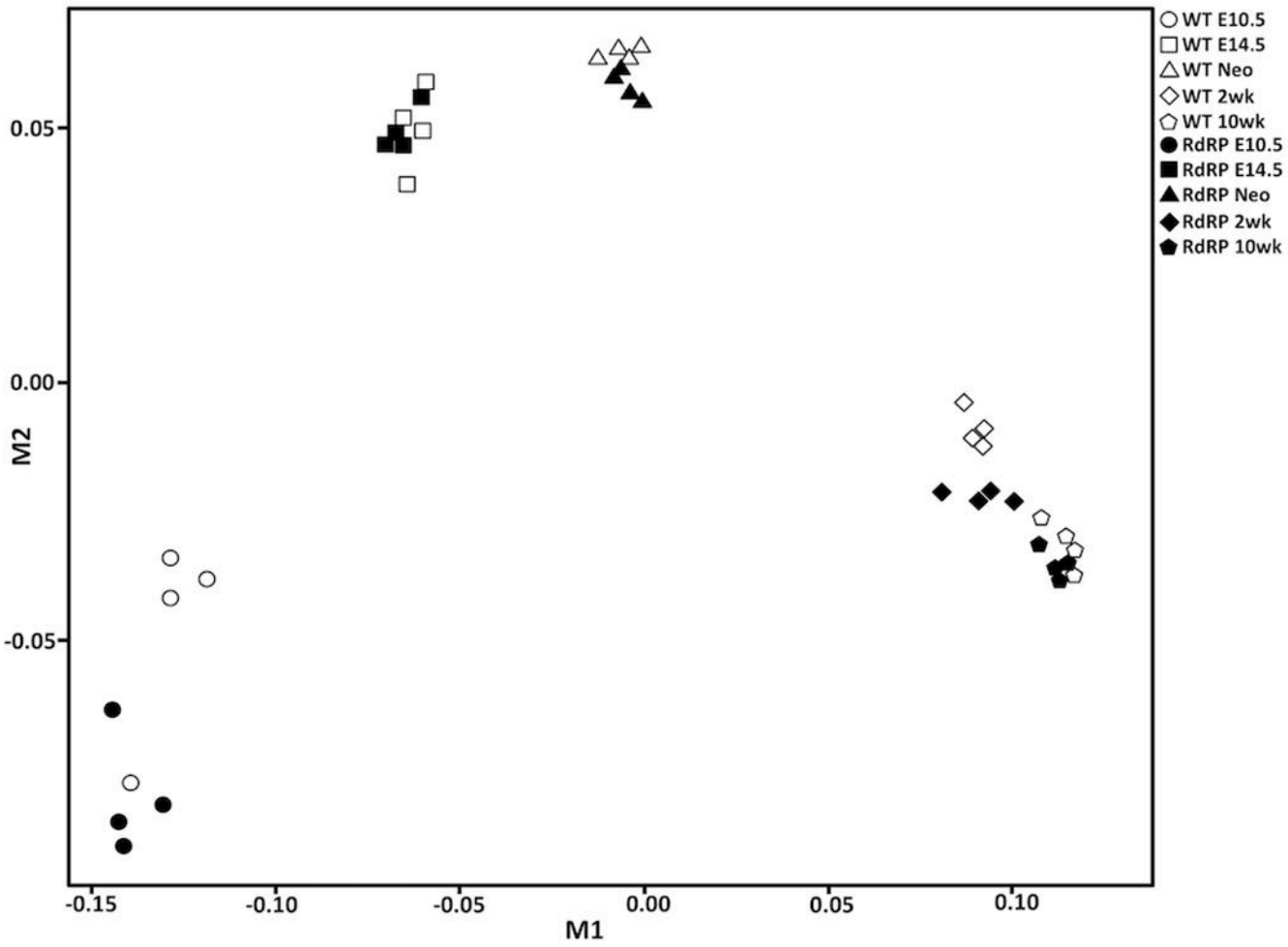

Fig 1. Multi-dimensional scaling plot for all RNA-seq samples

(4 biological replicates for each of 5 time points for both WT mice and RdRP mice). The MDS plot was generated using CummeRbund. This dimensionality reduction method clusters samples based on gene expression profile, such that samples with more similar gene expression profiles cluster closer together in plot space and samples with more divergent gene expression profiles will cluster farther apart.

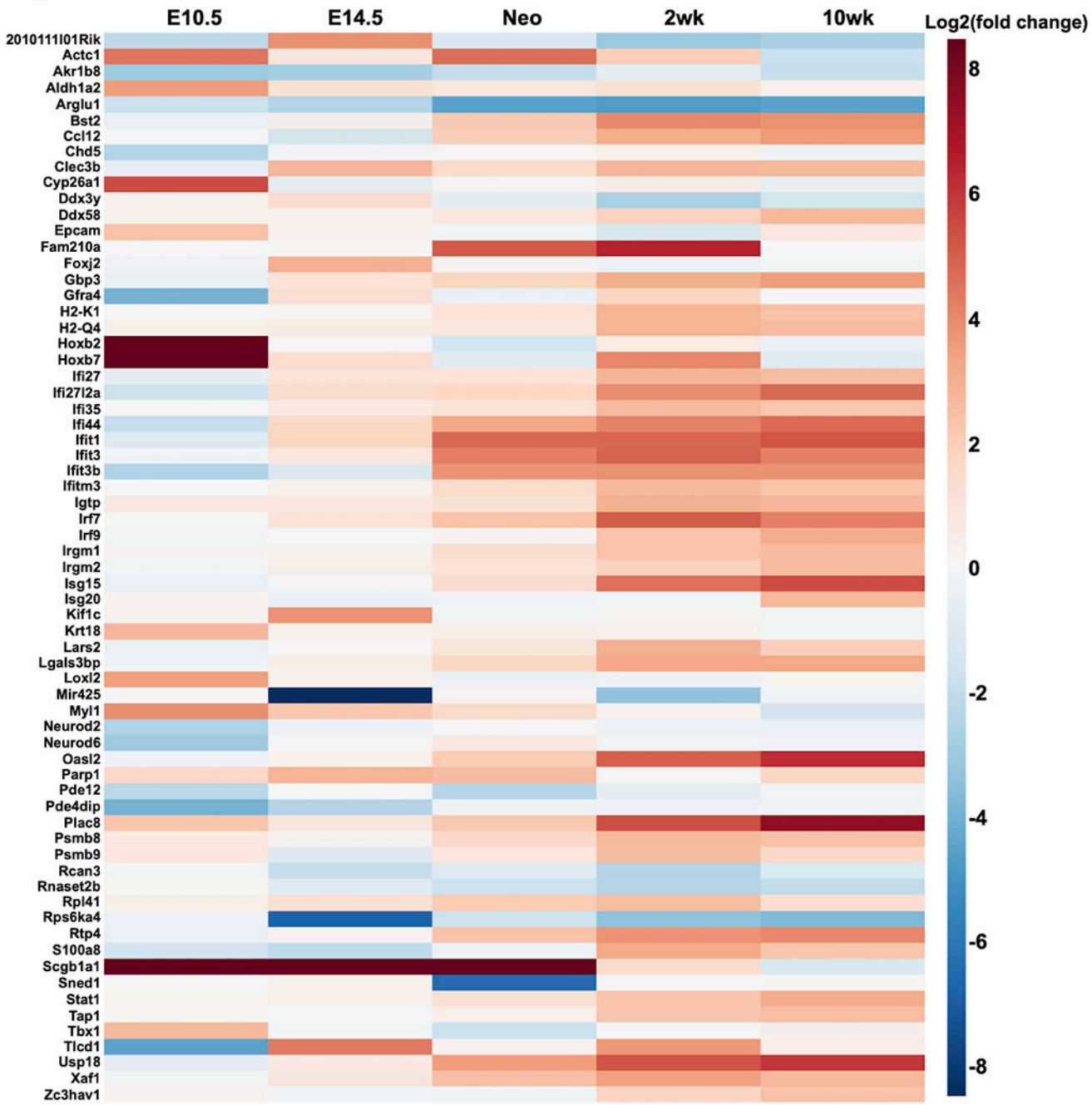

Fig 2. Heatmap depicting average Log_2(fold change) in RdRP relative to WT mice for each time point.

Only genes that represent known ISGs, based on matches to the Interferome Database, and that were upregulated or downregulated by at least 5-fold in at least one of the time points are shown. Positive Log_2(fold change) in red indicates upregulation in RdRP mice relative to WT mice and negative Log_2(fold change) in blue indicates downregulation in RdRP mice relative to WT mice.

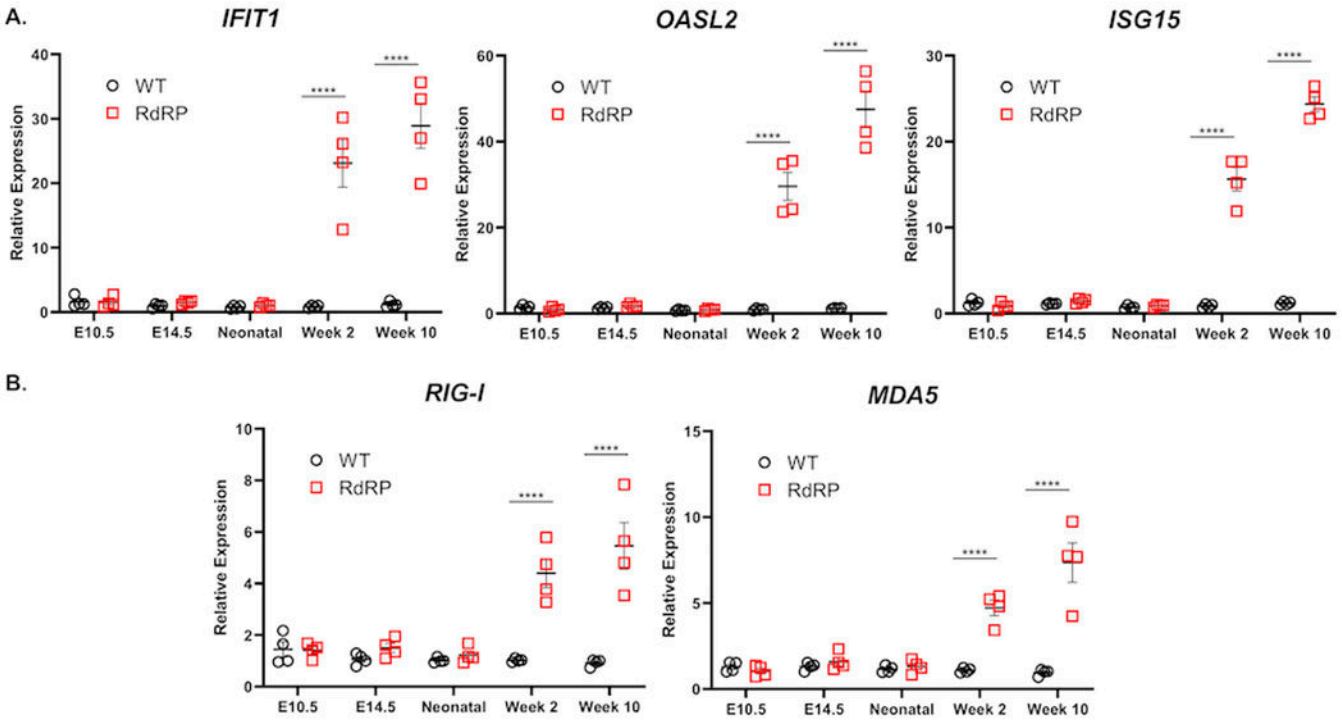

Fig 3. RT-qPCR for 5 representative genes in the RdRP relative to the WT mouse brain.

(A) *Ifit1*, *Oasl2*, and *Isg15*, (B) *Ddx58* (RIG-I), and *Ifih1* (MDA5) expression as measured by qPCR. Y-axes show mRNA fold change for each ISG in RdRP mice and WT mice at each time point relative to *Gapdh* mRNA levels. Black = WT control mice, Red = RdRP mice. Data are represented as mean ± SEM of four biological replicates, relative to endogenous *Gapdh* mRNA. Data were analyzed using a 2-way ANOVA where ****$p<0.0001$.

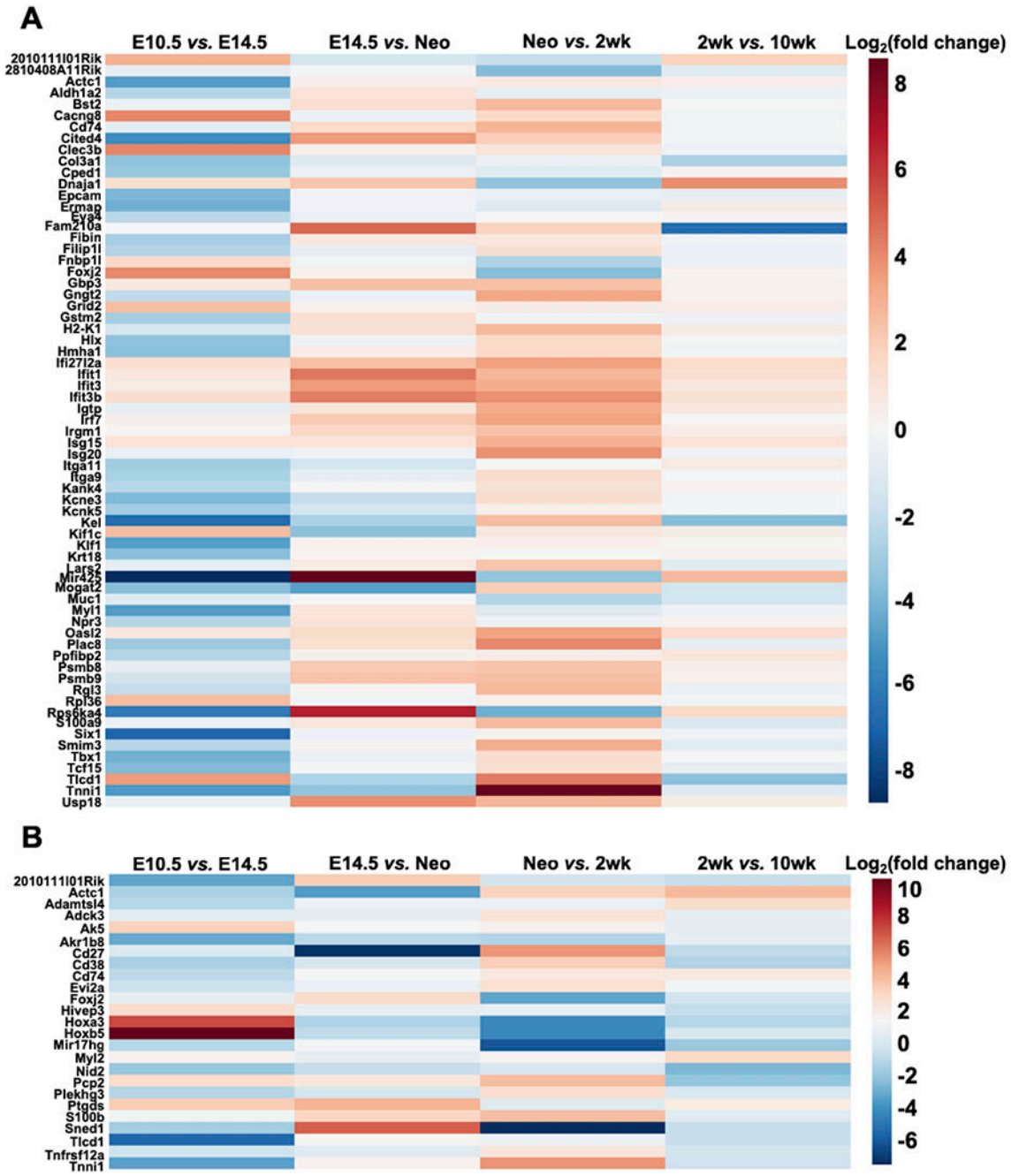

Fig 4. Heatmap depicting average Log$_2$(fold change) across the time series.

(A) RdRP mice across the time series. (B) WT mice across the time series. Here, gene expression changes for a given time point are quantified relative to the immediately previous time point. Only genes that represent known ISGs, based on matches to the Interferome Database, and that were upregulated or downregulated by at least 5-fold in at least one time point comparison are shown. Positive Log$_2$(fold change) in red indicates upregulation in a given time point relative to the previous time point and negative Log$_2$(fold change) in blue indicates downregulation in a given time point relative to the previous time point.

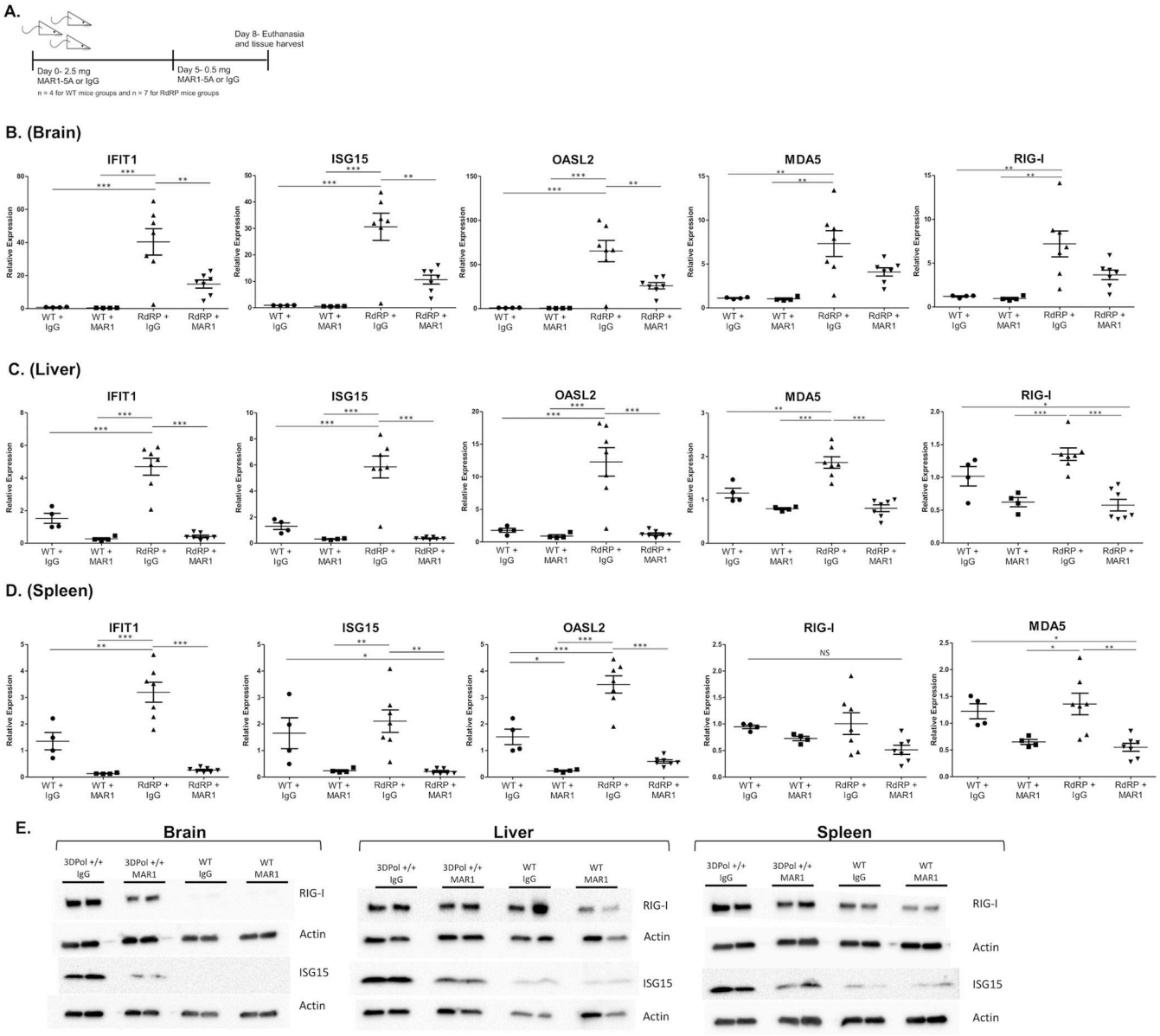

Fig 5. Administration of MAR1-5A anti-IFNAR neutralizing antibody to WT and RdRP mice.

(A) Antibody administration layout. Animals were intraperitoneally injected with MAR1–5A or control IgG on day 0 (2.5 mg) and day 5 (0.5 mg). Animals were euthanized for tissue harvest at day 8 post initial injection. N= 4 for all WT mice groups and n = 7 for all RdRP mice groups. (B) Brain, (C) liver, and (D) spleen qPCR for expression of *Ifit1*, *Isg15*, *oasL2*, *Ddx58* (RIG-I), and *ifih1* (MDA5) for animals treated as in (A). Data were analyzed using the $\Delta\Delta C_t$ method for gene expression relative to *Gapdh*. Statistical analysis utilized a 1-way ANOVA with a Tukey's test to determine significance thresholds where *$p < 0.05$, **$p < 0.01$, ***$p < 0.001$, and ****$p < 0.0001$. (E) Western blot for RIG-I, ISG15, and Actin of brain, liver, and spleen lysates from representative mice from (A). Protein input was

normalized by Bradford reaction prior to loading. Samples were run separately for RIG-I and SIG; corresponding actin blot shown for each protein.

Table I.

Pairwise DEGs Summary.

Comparison	Upregulated	ISGs (%)	Downregulated	ISGs (%)	Total	ISGs (%)
E10.5 WT vs. RdRP	35	10 (28.6%)	11	7 (63.6%)	46	17 (37.0%)
E14.5 WT vs. RdRP	11	6 (54.5%)	5	2 (40.0%)	16	8 (50.0%)
Neonate WT vs. RdRP	16	3 (18.8%)	6	3 (50.0%)	22	6 (27.3%)
2 wk WT vs. RdRP	40	30 (75.0%)	9	5 (55.6%)	49	35 (71.4%)
10 wk WT vs. RdRP	35	29 (82.9%)	3	1 (25.0%)	38	30 (78.9%)

Number of genes with at least 5-fold expression differences between WT and RdRP mice at each time point, and the number (percent) that represent known ISGs based on comparisons to the Interferome Database.

Table II.

Pairwise Canonical Pathways.

Comparison	Canonical Pathways	Category	−log(p-value)	z-score	ACT/IN	Upstream Regulators
E10.5 WT vs. RdRP	Actin Cytoskeleton Signaling	Organismal Growth and Development	4.36	2.24	ACT	NA
	ILK Signaling	Cellular Growth, Proliferation and Development	6.04	2.45	ACT	NA
	Regulation of Actin-based Motility by Rho	Neurotransmitters and Other Nervous System Signaling	4.79	2.00	ACT	NA
	RhoA Signaling	Intracellular and Second Messenger Signaling	4.25	2.00	ACT	NA
	RhoGDI Signaling	Intracellular and Second Messenger Signaling	3.65	−2.00	IN	NA
	Signaling by Rho Family GTPases	Intracellular and Second Messenger Signaling	3.07	2.00	ACT	NA
E14.5 WT vs. RdRP	NA	NA	NA	NA	NA	NA
Neo WT vs. RdRP	NA	NA	NA	NA	NA	NA
2wk WT vs. RdRP	Interferon Signaling	Cellular Immune Response; Cytokine Signaling	12.50	2.45	ACT	**EIF2AK2**, **IRF7**, **Irgm1**, **STAT1**
10wk WT vs. RdRP	Interferon Signaling	Cellular Immune Response; Cytokine Signaling	13.60	2.45	ACT	**EIF2AK2**, **IRF7**, **Irgm1**, **STAT1**, **STAT2**

Ingenuity Pathway Analysis (IPA) Canonical Pathways with significant Benjamini-Hochberg corrected p-values of overlap and activation z-scores in RdRP mice relative to WT mice within each of the 5 time points. Positive z-scores ≥ +2 indicate predicted activation and negative z-scores ≤ −2 indicate predicted inhibition. Upstream Regulators were predicted using IPA requiring at least 2-fold expression differences and a significant activation z-score. IPA Predicted Upstream Regulators are genes known to regulate a given pathway and/or one or more molecules in a pathway, those included had significant Benjamini-Hochberg corrected p-values of overlap and were differentially expressed in our dataset. Upstream Regulators in **bold** represent known ISGs. “NA” indicates comparisons for which there were no significantly activated or inhibited Canonical Pathways or DE Upstream Regulators.ACT: Activated. IN: Inhibited.

Table III.

Pairwise Functional Enrichment.

IPA Diseases and Biological Functions			
Comparison	**Diseases or Functions Annotation**	**p-value**	**z-score**
E10.5 RdRP relative to WT	Hypoplasia of organ	7.61E-06	−2.77
	Neonatal death	4.36E-04	−2.41
	Organismal death	4.55E-05	−2.88
	Perinatal death	3.74E-04	−2.59
E14.5 RdRP relative to WT	NA	NA	NA
Neo RdRP relative to WT	NA	NA	NA
2wk RdRP relative to WT	Bacterial Infections	5.14E-10	−2.18
	Immune response of cells	1.26E-05	2.18
	Infection of mammalia	6.65E-08	−2.73
	Morbidity or mortality	1.98E-03	−2.28
	Organismal death	5.05E-03	−2.55
	Quantity of IL-12 in blood	5.45E-07	−2.00
	Viral Infection	2.57E-07	−2.19
10wk RdRP relative to WT	Immune response of cells	7.30E-05	2.18
	Infection of mammalia	1.16E-10	−2.44
	Leukocyte migration	1.00E-02	2.34
	Migration of cells	4.73E-02	2.70
	Organismal death	4.86E-02	−2.23
	Quantity of IL-12 in blood	1.43E-07	−2.00
	Replication of vesicular stomatitis virus	4.05E-08	−2.11
	Viral Infection	3.24E-06	−2.87
DAVID GO enrichment			
Comparison	**GO Term**	**p-value**	**Fold.**
E10.5 RdRP relative to WT	anterior/posterior pattern specification	1.89E-06	31.50
	cardiac muscle contraction	1.11E-02	36.75
	cellular response to retinoic acid	3.17E-05	40.71
	embryonic skeletal system morphogenesis	1.43E-02	32.07
	multicellular organism development	4.08E-06	6.43
	neural crest cell development	2.88E-02	77.83
	positive regulation of transcription from RNA polymerase II promoter	1.34E-02	4.43
	regulation of transcription, DNA-templated	2.00E-04	3.48
	retinoic acid receptor signaling pathway	2.91E-02	73.50

IPA Diseases and Biological Functions			
Comparison	**Diseases or Functions Annotation**	**p-value**	**z-score**
	transcription, DNA-templated	2.21E-05	4.21
	DNA binding	1.74E-04	3.88
	RNA pol II core promoter proximal region sequence-specific DNA binding	3.11E-03	8.72
	sequence-specific DNA binding	2.35E-04	7.07
	transcription factor activity, sequence-specific DNA binding	1.94E-04	6.08
E14.5 RdRP relative to WT	NA	NA	NA
Neo RdRP relative to WT	ribosome	1.96E-02	26.15
	intracellular ribonucleoprotein complex	4.52E-02	15.36
	structural constituent of ribosome	2.09E-02	20.33
2wk RdRP relative to WT	cellular response to interferon-alpha	1.50E-02	105.13
	cellular response to interferon-beta	5.73E-06	61.54
	defense response to virus	1.74E-04	17.63
	immune system process	2.44E-07	13.18
	innate immune response	2.01E-04	9.46
	response to interferon-beta	9.59E-03	140.17
	response to virus	1.46E-04	30.04
10wk RdRP relative to WT	antigen processing and presentation	2.17E-03	39.39
	antigen processing and presentation of endogenous peptide antigen via MHC I, ER, TAP-dependent	2.13E-03	177.27
	antigen processing and presentation of exogenous peptide antigen via MHC I, TAP-dependent	1.78E-02	53.18
	antigen processing and presentation of peptide antigen via MHC class I	7.80E-04	59.09
	cellular response to interferon-alpha	3.24E-03	132.96
	cellular response to interferon-beta	4.54E-09	90.80
	defense response	4.74E-05	27.51
	defense response to virus	7.74E-10	31.85
	immune system process	2.88E-13	20.83
	innate immune response	1.03E-06	13.30
	negative regulation of viral genome replication	9.83E-06	83.10
	response to interferon-beta	1.22E-05	236.37
	response to interferon-gamma	1.44E-02	61.36
	response to virus	1.80E-10	56.98
	endoplasmic reticulum exit site	9.02E-03	91.31
	Golgi apparatus	4.81E-02	3.89
	Golgi medial cisterna	9.59E-03	102.05
	MHC class I protein complex	1.88E-04	144.57
	phagocytic vesicle membrane	2.62E-03	49.22
	beta-2-microglobulin binding	7.74E-03	125.81

IPA Diseases and Biological Functions			
Comparison	**Diseases or Functions Annotation**	**p-value**	**z-score**
	peptide antigen binding	1.14E-04	60.58
	RNA binding	7.04E-03	5.59
	T cell receptor binding	6.77E-03	116.83
	TAP binding	4.20E-03	204.45

Top panel: Enriched IPA Diseases and Biological Functions with significant activation z-scores in RdRP relative to WT mice at each time point. Bottom panel: enriched GO terms (DAVID) and fold enrichment (Fold) in RdRP relative to WT mice. P-values are Benjamini-Hochberg corrected. “NA” indicates no significant enrichment.

Table IV.

Timeseries DEGs Summary.

WT and RdRP	Upregulated	ISGs (%)	Downregulated	ISGs (%)	Total	ISGs (%)
E10.5 vs. E14.5	231	76 (32.9%)	96	40 (41.7%)	327	116 (35.5%)
E14.5 vs. Neo	34	17 (50.0%)	8	1 (12.5%)	42	18 (42.9%)
Neo vs. 2wk	243	108 (44.4%)	74	31 (41.9%)	317	139 (43.8%)
2wk vs. 10wk	5	3 (60.0%)	7	2 (28.9%)	12	5 (41.7%)
RdRP-only	**Upregulated**	**ISGs (%)**	**Downregulated**	**ISGs (%)**	**Total**	**ISGs (%)**
E10.5 vs. E14.5	27	7 (25.9%)	95	31 (32.6%)	122	38 (31.3%)
E14.5 vs. Neo	11	3 (27.3%)	7	2 (28.9%)	18	5 (27.8%)
Neo vs. 2wk	44	22 (50.0%)	17	3 (17.6%)	61	25 (41.0%)
2wk vs. 10wk	2	1 (50.0%)	8	2 (25.0%)	10	3 (30.0%)
WT-only	**Upregulated**	**ISGs (%)**	**Downregulated**	**ISGs (%)**	**Total**	**ISGs (%)**
E10.5 vs. E14.5	14	3 (21.4%)	7	3 (42.9%)	21	6 (28.9%)
E14.5 vs. Neo	9	5 (55.5%)	3	1 (33.3%)	12	6 (50.0%)
Neo vs. 2wk	14	6 (42.9%)	21	3 (14.3%)	35	9 (25.7%)
2wk vs. 10wk	17	5 (29.4%)	8	1 (12.5%)	25	6 (24.0%)

The number of upregulated, downregulated, and total DEGs in the timeseries analyses for RdRP mice and WT mice. The top panel contains DEGs that showed consistent directional changes in expression over time in both WT mice and RdRP mice. The middle panel contains DEGs that were only differentially expressed in a given time point comparison in RdRP mice. The bottom panel contains DEGs that were only differentially expressed in a given time point comparison in WT mice. The numbers (percent) of known ISGs in each category, based on comparisons to the Interferome Database are also shown.

Table V.

Timeseries Canonical Pathways.

Comparison		Ingenuity Canonical Pathways	Category	−log(p-value)	z-score	ACT/IN	Upstream Regulators
RdRP	**E10.5 vs. E14.5**	α-Adrenergic Signaling	Intracellular and Second Messenger Signaling	1.65	2.24	ACT	BVHT
		CDK5 Signaling	Cell Cycle Regulation;Neurotransmitters and Other Nervous System Signaling	2.25	2.53	ACT	NA
		Cell Cycle: G2/M DNA Damage Checkpoint Regulation	Cell Cycle Regulation;Ingenuity Toxicity List Pathways	2.00	2.24	ACT	**E2F3**, TBX2
		Ephrin Receptor Signaling	Neurotransmitters and Other Nervous System Signaling;Organismal Growth and Development	1.45	2.53	ACT	CCN1, **REST**
		GNRH Signaling	Neurotransmitters and Other Nervous System Signaling	3.19	2.33	ACT	CCN1, CCN2, **REST**
		ILK Signaling	Cellular Growth, Proliferation and Development	2.95	−3.50	IN	BVHT, CCN1, CCN2, **E2F3**, **PDGFC**, **REST**
		Mitotic Roles of Polo-Like Kinase	Cell Cycle Regulation	1.96	−2.24	IN	**E2F3**, TBX2
		RhoA Signaling	Intracellular and Second Messenger Signaling	1.77	−2.33	IN	BVHT, **NFE2L2**, **PDGFC**
	E14.5 vs. Neo	ERK/MAPK Signaling	Cancer;Intracellular and Second Messenger Signaling	2.43	2.24	ACT	NA
	Neo vs. 2wk	Interferon Signaling	Cellular Immune Response; Cytokine Signaling	2.14	2.00	ACT	CREBBP, CREBPA, **EIF2AK2**, **IRF7**, **Irgm1**, **MAVS**, **SPI1**
		Neuroinflammation Signaling Pathway	Cellular Immune Response;Disease-Specific Pathways;Neurotransmitters and Other Nervous System Signaling	5.34	2.00	ACT	**CHUK**, CREBBP, CREBPA, **EIF2AK2**, **IRF7**, **Irgm1**, **MAP2K1**, **SOX4**, **SPI1**
	2wk vs. 10wk	NA	NA	NA	NA	NA	NA
WT	**E10.5 vs. E14.5**	Amyotrophic Lateral Sclerosis Signaling	Disease-Specific Pathways;Neurotransmitters and Other Nervous System Signaling	4.22	2.65	ACT	NA
		cAMP-mediated signaling	Intracellular and Second Messenger Signaling	2.01	3.00	ACT	NA
		Gαq Signaling	Intracellular and Second Messenger Signaling	1.39	2.24	ACT	NA
		GP6 Signaling Pathway	Cellular Stress and Injury	7.62	−2.67	IN	NA
		Neuroinflammation Signaling Pathway	Cellular Immune Response;Disease-Specific Pathways;Neurotransmitters and Other Nervous System Signaling	3.92	2.65	ACT	NA
	E14.5 vs. Neo	Sperm Motility	Organismal Growth and Development	3.13	2.00	ACT	NA

Comparison		Ingenuity Canonical Pathways	Category	−log(p-value)	z-score	ACT/IN	Upstream Regulators
	Neo vs. 2wk	α-Adrenergic Signaling	Intracellular and Second Messenger Signaling	1.56	2.00	ACT	NA
		3-phosphoinositide Biosynthesis	Phospholipid Biosynthesis	1.50	2.83	ACT	**EOMES**
		cAMP-mediated signaling	Intracellular and Second Messenger Signaling	2.03	2.53	ACT	NA
		D-myo-inositol-5-phosphate Metabolism	Phospholipid Biosynthesis	1.53	2.65	ACT	**EOMES**
		Neuropathic Pain Signaling In Dorsal Horn Neurons	Neurotransmitters and Other Nervous System Signaling	1.72	2.45	ACT	NA
		RhoA Signaling	Intracellular and Second Messenger Signaling	1.58	2.24	ACT	NA
	2wk vs. 10wk	NA	NA	NA	NA	NA	NA

Ingenuity Pathway Analysis (IPA) Canonical Pathways with significant Benjamini-Hochberg corrected p-values of overlap, and activation z-scores across the time series that differ between RdRP mice (top) and WT mice (bottom). Pathways with positive z-scores ≥ +2 indicate predicted activation, and pathways with negative z-scores ≤ −2 indicate inhibition. IPA Predicted Upstream Regulators are genes known to regulate a given pathway and/or one or more molecules in a pathway, those included had significant Benjamini-Hochberg corrected p-values of overlap and were differentially expressed in our dataset and exhibited different expression patterns in the RdRP vs. WT timeseries. Upstream Regulators in **bold** represent known ISGs. “NA” indicates comparisons for which there were no significantly activated or inhibited Canonical Pathways or DE Upstream Regulators. ACT: Activated. IN: Inhibited.